Dear Marcel van der Meer,

thank you for serving as handling author of our manuscript and for the constructive feedback. Please find attached the revised versions of the author responses to referee #1 and #2 as well as the manuscript and the supplements (track change marked versions).

Best regards,
Johannes Hepp

Revised reply to Referee #1

by Johannes Hepp, Michael and Roland Zech & co-authors

We are grateful to anonymous Referee #1 for her/his constructive suggestions helping to improve our manuscript. Please find our replies to the individual comments below.

Major issues:

1) The brGDGT calibration presented here is of limited use, since the study uses an outdated method to measure brGDGTs and does not distinguish between the 5 methyl and 6 methyl compounds. Hepp et al. thus calibrate indices (CBT and MBT') that have fallen out of favor and been replaced by the more robust CBT' and MBT5Me indices. The new indices and new methods developed by De Jonge et al. (GCA, 2014, doi: 10.1016/j.gca.2014.06.013) and Hopmans et al. (Organic Geochemistry, 2016, doi: 10.1016/j.orggeochem.2015.12.006) are not even mentioned in the text, and the limitations of the brGDGT data presented here are not acknowledged. Without reanalyzing these samples with a method that resolves all isomers, I fear that the present sample set has limited value for the calibration of brGDGT-based proxies.

→ Referee #1 is right in his/her statement that the GDGT data presented in our manuscript were not acquired based on the up-to-date method. During revision, we therefore explicitly emphasize that meanwhile new indices and methods were developed (including citations). We would still see a high value of having our GDGT dataset published. De Jonge et al. (2014) presented a new HPLC method which enables the separation for the brGDGTs with m/z 1036, 1034 and 1032, 1050, 1048 and 1046 into 6-methyl and 5-methyl stereoisomers. The old method did not allow such a separation (Zech et al., 2012b) thus in the calibration often the sum of 6 and 5-methlyted brGDGTs was used because the shoulders of the peaks could not be identified in each case (see and compare De Jonge et al., 2014; Peterse et al., 2012). This introduce scatter to the MBT´-CBT-based MAT reconstructions and can cause a correlation between pH and MBT` (for more details see De Jonge et al., 2014). The authors moreover show that the 6-methyl brGDGTs are ubiquitous abundant in soils from all over the world. However, they also compare reconstructed MAT values based MBT´-CBT calibration (Peterse et al., 2012) and their new developed MAT_{mr} calibration and state that they plot around a 1:1 relationship. They furthermore state that only for arid areas a strong deviation can be obtained. Finally, they conclude that the use of the new developed calibrations will improve the MAT and pH reconstructions for dry conditions/areas. Because our study transect spans form southern Germany to southern Sweden, representing temperate and humid climate conditions, we argue that the usage of the older HPLC method do not introduce a systematic error in our reconstructions. Still, a higher variability/scatter is associated with the calibration of Peterse et al. (2012) and therefore present in our MAT and pH reconstructions. However, we firstly compared our data only to those of Peterse et al. (2012), and we secondly prevented an over-interpretation of our data. This discussion is now included as a separate discussion chapter in the revised version of the manuscript.

2) There are some big assumptions in the proposed approach for reconstructing relative humidity using paired δ2H values of n-alkanes and δ18O values of sugars. In particular, the assumption that biosynthetic fractionation for these compounds is constant is contradicted by lots of existing work, which is briefly mentioned by the authors in their discussion. Figure 8 is not a very good advertisement for the utility of the paired δ2H-alkane/δ18O sugar approach, and the lack of correlation suggests that some of the many assumptions that go into this method are not valid. This paired approach has not caught on beyond the Zech group, and the data presented here suggests that it may not be useful as presently conceived. The authors state they have shown the "great potential" for this proxy. I remain unconvinced by the data and analysis shown here.

→ We accept that Referee #1 remains unconvinced by our coupled $\delta^2H_{n\text{-alkane}}$-$\delta^{18}O_{sugar}$ biomarker approach. We moreover we (i) agree, (ii) are aware and (iii) explicitly state that the assumption of constant biosynthetic fraction is likely a major uncertainty of our approach. Still we are convinced that the 'opening of the second dimension' by our group is a cutting-edge step forward and more promising than focusing on $\delta^2H_{n\text{-alkane}}$ alone. The reason for other working groups not having caught on the coupled approach might have to be seen, in our opinion, in the uniqueness of compound-specific $\delta^{18}O$ analyses: according to our knowledge, only 3 working groups world-wide have respective experience/publication records. Still, we would be delighted to see the coupled approach being tested or applied by other groups, readily in cooperation with us. Still we acknowledge that focusing on $\delta^2H_{n\text{-alkane}}$ hast the advantage that a lot of research was done and many working groups around the world published results during the last years. The coupling is still work in progress but we think we have to start somewhere and this introduces also (new) uncertainties for sure, but is still worth to publish and start the process of proxy improvement via scientific discussions with this.

Possibly, Referee #1 misunderstood Fig. 8. No correlation for the data points shown in Fig. 8 are to be expected. We clarified in our revision that Fig. 8 illustrates the 'concept of the coupled $\delta^2H_{n\text{-alkane}}$-$\delta^{18}O_{sugar}$ biomarker approach'. This conceptual figure illustrates (together with Fig. 9) that $\delta^2H/\delta^{18}O_{prec}$ values reconstructed by the coupled approach are more accurate than δ^2H_{prec} values reconstructed using $\delta^2H_{n\text{-alkane}}$ alone. Moreover, Fig. 10 illustrates that reconstructed RH values under deciduous forest sites and grassland sites are quite well in accordance with RH values of climate stations, thus indeed demonstrating the great potential of the coupled approach.

3) The writing is in places unclear and difficult to follow. I have noted a few of these instances in my technical corrections, but the manuscript would benefit from more careful editing.

→ We insure a technical and grammatical improvement for the revised version of the manuscript.

Specific comments:

Line 110: This adds up to more than 16, some sites were considered to be more than one of these categories? Would be good to rewrite to clarify

→ Following the recommendation of Referee #1 we will restructure this sentence. The revised version will read: “In November 2012, we collected 29 topsoil samples (0-5 cm depth) from 16 sites along a transect from Southern Germany to Southern Sweden (Fig. 1A). We distinguished between coniferous forest (con, n = 9), …”.

Line 114: Was there a threshold for what was considered "close-by"?

→ We agree with Referee #1 that this was not obvious so far in the manuscript and especially not in the supplementary material where the longitude, latitude and altitude were provided for the climate stations (Tab. S2) but not for the locations/sites. In the revised manuscript, we will add the respective characteristics to Tab S1.

Line 133: Machine learning techniques like random forest aren’t so commonly used in Biogeosciences and it would be helpful to provide more details here. How many trees did you use? How was data partitioned into training and testing sets? What metric was used to assess model performance? What was the minimum number of samples in the terminal nodes? What was the maximum number of terminal nodes? What variables ended up being ranked as most important (could be useful to show a plot of ranked variable importance in the supplemental materials)?

→ As suggested, we will add a supplementary method description part and refer to it in the text.

Line 136: Why wasn’t it possible? Lack of measured data for a robust training data set? Please specify

→ Because no precipitation isotope data was available for the Danish and Swedish sites.

Lines 128-139: How did the calculated values you obtained for the German sites compare to OIPC? What is your evidence for your approach providing superior estimates of precip isotopes than OIPC? OIPC is obviously not perfect, but as written, we have no evidence to evaluate if your results are any more accurate. There is also no discussion of the implications of using one target for precip isotopes in the southern half of your transect and a different one in the northern half.

→ Please allow us to refer to the (cited) Diploma Thesis of Schlotter (2007): there are numerous reasons mentioned already in the introduction highlighting that OPIC is probably not the most robust estimator for middle and high latitudes. That’s why we used our own regionalization where it was possible.

Section 2.3.1: No internal standard was added? How do you account for losses of brGDGTs during sample handling?

→ We used standard laboratory procedure for GDGT sample preparation. The internal standard was, as written, added before the measurements. A correction for GDGT losses during sample preparation is therefore not possible.

Lines 165-171: This is not the most current method used for robust brGDGT analysis (see Hopmans et al., Organic Geochemistry, 2016. DOI: 10.1016/j.orggeochem.2015.12.006). Does your method allow for 5’

and 6' methyl brGDGTs to be distinguished from one another? If not, severely diminishes the accuracy of results. Based on the results that are shown, it seems like this method does not distinguish the different isomers.

→ That's correct. Please see our reply to major issue 1.

Lines 172-173: how was the pH measured?

→ We will include the information that a pH meter was used.

Section 2.3.2: Were the n-alkanes quantified prior to measuring their stable isotopes?

→ Yes, namely by Schäfer et al. (2016). We therefore added the following sentence in the section: "For more details about *n*-alkane quantification the reader is referred to Schäfer et al. (2016). ".

Also, please briefly describe the operating conditions of the GC-pyr-IRMS (or cite another publication that used an identical method and provides all the relevant details)

→ As suggested, we added now in the revised version of the manuscript a reference (Christoph et al., 2019), in which the method is described in more detail and we added that the ^{2}H pyrolysis reactor temperature was kept at 1420 °C.

Line 199: It is not clear how you had 29 samples from 16 sites. Were some of the sites sampled in duplicate?

→ We will clarify during revision that 29 samples were collected from 16 sites. These are, however, no duplicates, but rather different dominant vegetation types (see reply above).

Lines 211-221: The more robust indicator of soil pH is CBT' and the more robust indicator of soil temperature is MBT5me (De Jonge et al., GCA, 2014, DOI:10.1016/j.gca.2014.06.013).

→ See our reply to major issue 1.

Lines 227-229: A number of papers have shown that ebio is not constant and different among plant types and seasonally. See for example Feakins & Sessions 2010 (cited previously), Eley et al., GCA, 2014 (DOI: 10.1016/j.gca.2013.11.045), Cormier et al., New Phytologist, 2018 (DOI: 10.1111/nph.15016).

→ That's true and especially important when only $\delta^{2}H_{n\text{-alkane}}$ is used to reconstruct $\delta^{2}H_{\text{leaf-water}}$. Nevertheless, we emphasize in our manuscript that ε_{bio} is a major uncertainty in our coupled approach, too. At the same time, it's exactly such uncertainties why we need climate transect calibration studies as the one presented here for Europe.

Lines 383-385: are these concentrated weighted means? That is what is typically used to compare d2H values of n-alkanes where not all homologues are present in all samples

→ We used here mean values, because the areas and concentrations where not determined during isotope measurements.

Line 395: I think you mean "unenriched xylem water"?

→ Yes, changed.

Lines 431-432: This is not particularly convincing, the reconstructed precipitation isotopes are not correlated with the GIPR/OIPC precipitation isotopes. No evidence is provided to show that this approach is any better than the most up to date methods for obtaining precipitation isotopes from leaf wax n-alkane isotopes alone. For example, how do your results compare to the predictions from the proxy system model developed by Konecky et al. (JGR-Biogeoscience, 2019, DOI: 10.1029/2018JG004708)? Maybe your approach is better, but you need to prove this by providing a direct comparison, rather than just telling us

→ Please note that we do not necessarily expect a good correlation of our reconstructed $\delta^2H/\delta^{18}O_{prec}$ values with the GIPR/OIPC data, but rather a good (accurate) match on the 1:1 line. Nevertheless, many thanks for pointing us to the new publication by Konecky et al. (2019). While we will readily include a respective citation, we think that a direct comparison of our approach with the one suggested by Konecky et al. (2019) would be beyond the scope of our manuscript.

Lines 448-450: If this was the case, wouldn't you expect all the coniferous sites to be biased in the same direction? Instead, they are evenly distributed above and below the 1:1 line

→ No, please see Fig. 9: we do not see that the coniferous sites are evenly distributed around the 1:1 line. Except for one data point, they are clearly below the 1:1 line.

Line 454: Is this signal damping correction shown anywhere? How would this work practically in sediments?

→ No, sorry. This signal damping correction is not shown or quantified in this manuscript. This would require a quantitative estimation of the contribution of grass vegetation to the total biomass pool in the topsoil. For an example how such a correction can be applied to lake sediments please see e.g. Hepp et al. (2019, CP).

Lines 467-468: Actually, there are plenty of n-alkanes in roots and they have very different H isotopic composition than in leaves. See work from Guido Wiesenberg's group and Gamarra and Kahmen. I'm also confused about what you are referring to as "the discussion". There is not a separate discussion section to this manuscript.

→ Changed to "Zech et al. ,2012b and the discussion therein". We do not agree and we are not aware of any new studies showing that *n*-alkanes are produced in large amounts by roots in comparison to leaves. Recent studies show (e.g. Gamarra and Kahmen, 2015) that root *n*-alkane concentration is always the lowest compared to the other plant tissues sampled.

Lines 489-494: Not stated here is that there is no correlation between the reconstructed and measured RH values. This suggests that this approach for reconstructing RH is not particularly useful Line 565: The data in the paper is not very convincing that there is great potential for the coupled d2H n-alkane d18O sugar approach

→ We think this is connected to the low range of measured RH values along this European climate transect and the uncertainties of the coupled approach for reconstructing RH values.

Therefore, the lack of a respective correlation is explainable. Please compare a similar climate transect study by Tuthorn et al. (2015, BG) where the RH range is much larger and where indeed a significant correlation can be found. For this European transect study here, the usefulness of the coupled approach for reconstructing RH values should be rather inferred from the quite well 1:1 match for deciduous forest sites and grassland sites (cf. Fig. 9). The RH underestimation for coniferous forest sites can be easily explained with the extremely low *n*-alkane production of coniferous trees (see ll. 495-502).

Lines 566-567: I don't see evidence of this in your analysis, nor examples of how you would take vegetation into account when applying this proxy.

→ See for example Hepp et al. (2019).

Technical corrections and typing errors:

Lines 54-56: The way this sentence is written is confusing. Suggest rewriting as "Climate proxies based on molecular fossils, also known as biomarkers, have great potential...

→ Changed.

Line 56: don't need the comma after "particular"

→ Changed.

Line 59: "need to be known"?

→ Changed.

Line 61: It would be better to start this paragraph with a clear link back to the previous one

→ We now start the paragraph with "One famous and widely applied lipid biomarker group are terrestrial branched glycerol dialkyl glycerol tetraethers (brGDGTs). They are synthesized… and…"

Line 74: don't need commas before and after "it is known"

→ Changed.

Line 79: Again, some sort of transition would be helpful to begin this paragraph

→ We now start the paragraph with "Concerning paleohydrology proxies, compound-specific…"

Line 82: "all along the way" too wordy

→ Changed

Lines 93-94: "as well as concerning possible effects related to" awkward phrasing

→ Changed.

Figure 1: would be nice to have a legend on panel B or have the axis colors match the variable colors. At the moment we are left to guess that blue bars are precip and the red dots are temp, since this is not stated in the figure caption or the legend. Also would be nice to offset the panel letters with a () or . to break them apart from the title of the panel

→ Changed.

Line 180: No "the" needed in front of ETH

→ Changed.

Line 225: the n at the beginning of n-alkane should be italicized. Check throughout

→ Changed.

Line 234: Generally, figures should be numbered in the same order that they are referenced in the text

→ Checked and changed if necessary.

References

Christoph, H., Eglinton, T. I., Zech, W., Sosin, P. and Zech, R.: A 250 ka leaf-wax δD record from a loess section in Darai Kalon , Southern Tajikistan, Quaternary Science Reviews, 208, 118–128, doi:10.1016/j.quascirev.2019.01.019, 2019.

Gamarra, B. and Kahmen, A.: Concentrations and δ^2H values of cuticular *n*-alkanes vary significantly among plant organs, species and habitats in grasses from an alpine and a temperate European grassland, Oecologia, 178, 981–998, doi:10.1007/s00442-015-3278-6, 2015.

Hepp, J., Wüthrich, L., Bromm, T., Bliedtner, M., Schäfer, I. K., Glaser, B., Rozanski, K., Sirocko, F., Zech, R. and Zech, M.: How dry was the Younger Dryas? Evidence from a coupled δ^2H–$\delta^{18}O$ biomarker paleohygrometer applied to the Gemündener Maar sediments, Western Eifel, Germany, Climate of the Past, 15, 713–733, doi:10.5194/cp-15-713-2019, 2019.

De Jonge, C., Hopmans, E. C., Zell, C. I., Kim, J. H., Schouten, S. and Sinninghe Damsté, J. S.: Occurrence and abundance of 6-methyl branched glycerol dialkyl glycerol tetraethers in soils: Implications for palaeoclimate reconstruction, Geochimica et Cosmochimica Acta, 141, 97–112, doi:10.1016/j.gca.2016.03.038, 2014.

Konecky, B., Dee, S. G. and Noone, D. C.: WaxPSM: A Forward Model of Leaf Wax Hydrogen Isotope Ratios to Bridge Proxy and Model Estimates of Past Climate, Journal of Geophysical Research: Biogeosciences, 124, 2107–2125, doi:10.1029/2018JG004708, 2019.

Peterse, F., van der Meer, J., Schouten, S., Weijers, J. W. H., Fierer, N., Jackson, R. B., Kim, J. H. and Sinninghe Damsté, J. S.: Revised calibration of the MBT-CBT paleotemperature proxy based on branched tetraether membrane lipids in surface soils, Geochimica et Cosmochimica Acta, 96, 215–229, doi:10.1016/j.gca.2012.08.011, 2012.

Schlotter, D.: The spatio-temporal distribution of $\delta^{18}O$ and $\delta^{2}H$ of precipitation in Germany - an evaluation of regionalization methods, Albert-Ludwigs-Universität Freiburg im Breisgau. [online] Available from: http://www.hydrology.uni-freiburg.de/abschluss/Schlotter_D_2007_DA.pdf, 2007.

Tuthorn, M., Zech, R., Ruppenthal, M., Oelmann, Y., Kahmen, A., del Valle, H. F., Eglinton, T., Rozanski, K. and Zech, M.: Coupling $\delta^{2}H$ and $\delta^{18}O$ biomarker results yields information on relative humidity and isotopic composition of precipitation - a climate transect validation study, Biogeosciences, 12, 3913–3924, doi:10.5194/bg-12-3913-2015, 2015.

Zech, M., Kreutzer, S., Goslar, T., Meszner, S., Krause, T., Faust, D. and Fuchs, M.: Technical Note: *n*-Alkane lipid biomarkers in loess: post-sedimentary or syn-sedimentary?, Discussions, Biogeosciences, 9, 9875–9896, doi:10.5194/bgd-9-9875-2012, 2012a.

Zech, R., Gao, L., Tarozo, R. and Huang, Y.: Branched glycerol dialkyl glycerol tetraethers in Pleistocene loess-paleosol sequences: Three case studies, Organic Geochemistry, 53, 38–44, doi:10.1016/j.orggeochem.2012.09.005, 2012b.

Revised reply to Referee #2

by Johannes Hepp, Michael and Roland Zech & co-authors

GENERAL:

The topic of the manuscript is interesting and important as it deals with the evaluation of highly promising proxies used to reconstruct past environmental conditions. While the data produced are rare and are certainly worth publishing, the manuscript has severe flaws that prevent, in my opinion, its publication in this form.

→ While we are grateful to Referee #2 for her/his constructive suggestions helping to improve our manuscript (see our replies below).

MAJOR PROBLEMS:

A) While reading the manuscript, the connection between GDGT and the plant proxies (i.e. n-alkanes and hemicellulose) is not clear and seems disconnected as if from two separate manuscripts. Moreover, in the section 3.1 of the discussion, the GDGT data are presented in a way leading the readers to believe that these molecules are produced by plants.

→ Thank you for raising this issue. We think that approaches are based on biomarkers/molecular proxies and are used for paleoclimate reconstructions. Moreover, we clearly state and explain in the introduction and method sections how the applied biomarkers (GDGT´s as well as *n*-alkanes and sugars) are produced, how calculations are done and how the proxies can be interpreted. Please note that there are plenty of studies in the literature presenting both GDGT and $\delta^2H_{n\text{-alkane}}$ results in one publication. However, we will check the whole manuscript during revision in order to be clear about the origin of the presented biomarker proxies.

B) The other major point is that the authors suggest that it is "often" not feasible to disentangle between the evapotranspirative enrichment from the precipitation signal, but there is at least another well-established method to do so and published in Climate of the Past (see recent Sachse's group publications, e.g. A dual-biomarker approach for quantification of changes in relative humidity from sedimentary lipid D/H ratios, Climate of the Past, 2017). While this method should at least be mentioned, I also believe the method should be compared to help the readers understand the full set of tools available to study that issue. These two methods are very likely to be highly complementary.

→ Thank you for raising this issue, but please note that the 'dual biomarker approach' of Rach et al. (2017, CP) is not applicable to terrestrial (soil) samples/archives, it works only under lacustrine settings. For a critical evaluation and assessment of both approaches when applied to lacustrine paleoclimate archives, we kindly refer our readers to Hepp et al. (2019, CP) and to our replies to the referee and short comments (https://www.clim-past.net/15/713/2019/cp-15-713-2019-discussion.html).

SPECIFICS:

Line 298 to 303: This section is not clear due to some typos or mistakes, please reformulate.

→ Changed.

Line 389 to 407: While the difference of ebio is reported at the end of the section (around line 477 to 487), the possibility that a variable ebio could explain the different signals in different types of vegetation, beside the damping effect, is evacuated of the discussion. This should at least be discussed.

→ Changed.

Line 432: Is that referring to simply using isotope values of a single compound? What is that hitherto method (reference missing?)? I believe this brings us back to the problem B. The results would gain a lot to be compared with the updated tool box of proxies.

→ The sentence was slightly changed. See also our reply to 'major problem B'.

Line 444 to 458: The argumentation is not clear/convincing, please reformulate.

→ We deleted the respective sentence from the revised version of the manuscript.

Line 483-484: The idea of a variable ebio is well expressed in general, but references to some recent works is missing that shows even greater variability in n-alkane dD values under different metabolisms (e.g. Cormier et al, 2018 – New Phytologist, Tipple & Ehleringer 2018 – Oecologia, Cormier et al, 2019 – Oecologia)

→ Please note that we already included Cormier et al. (2018) in the actual version of the manuscript and that the fact is mentioned that ε_{bio} can range even larger when also the metabolic status of the plants is considered. However, we changed the respective sentence to: "The wide range in biosynthetic ^{2}H fractionation factors, which can be even larger, is therefore also related to the carbon and energy metabolism state of plants (Cormier et al., 2018).".

Line 490 to 494: Please reformulate, this section is not clear.

→ We changed the quoting of Fig. 10B.

Line 550: If the author are really considering a variable ebio, the damping effect can only potentially explain the different signals observed in different types of vegetation. Again, ebio should be part of the points because standing alone, they can induce confusion even if mentioned afterward.

→ You are right. Gao et al. (2014) and Liu et al. (2016) showed that the ε_{bio} of monocot plants could larger than those of dicots. This would therefore course a more negative apparent fractionation factor for grasses compared to trees. We observe that the apparent fractionation is indeed more negative for the grass sites compared to the forest sites. We will included a discussion about the indistinguishable effects of "signal damping" vs. variable ε_{bio} along with vegetation types in the respective parts of the manuscript.

References

Aichner, B., Ott, F., Słowiński, M., Noryśkiewicz, A. M., Brauer, A. and Sachse, D.: Leaf wax *n*-alkane distributions record ecological changes during the Younger Dryas at Trzechowskie paleolake (Northern Poland) without temporal delay, Climate of the Past Discussions, (March), 1–29, doi:10.5194/cp-2018-6, 2018.

Cormier, M.-A., Werner, R. A., Sauer, P. E., Gröcke, D. R., M.C., L., Wieloch, T., Schleucher, J. and Kahmen, A.: ^{2}H fractiontions during the biosynthesis of carbohydrates and lipids imprint a metabolic signal on the $\delta^{2}H$ values of plant organic compounds, New Phytologist, 218(2), 479–491, doi:10.1111/nph.15016, 2018.

Gao, L., Edwards, E. J., Zeng, Y. and Huang, Y.: Major evolutionary trends in hydrogen isotope fractionation of vascular plant leaf waxes, PLoS ONE, 9(11), doi:10.1371/journal.pone.0112610, 2014.

Hepp, J., Wüthrich, L., Bromm, T., Bliedtner, M., Schäfer, I. K., Glaser, B., Rozanski, K., Sirocko, F., Zech, R. and Zech, M.: How dry was the Younger Dryas? Evidence from a coupled $\delta^{2}H$–$\delta^{18}O$ biomarker paleohygrometer applied to the Gemündener Maar sediments, Western Eifel, Germany, Climate of the Past, 15, 713–733, doi:10.5194/cp-15-713-2019, 2019.

Liu, J., Liu, W., An, Z. and Yang, H.: Different hydrogen isotope fractionations during lipid formation in higher plants: Implications for paleohydrology reconstruction at a global scale, Scientific Reports, 6, 19711, doi:10.1038/srep19711, 2016.

Rach, O., Kahmen, A., Brauer, A. and Sachse, D.: A dual-biomarker approach for quantification of changes in relative humidity from sedimentary lipid D/H ratios, Climate of the Past, 13, 741–757, doi:10.5194/cp-2017-7, 2017.

Tuthorn, M., Zech, R., Ruppenthal, M., Oelmann, Y., Kahmen, A., del Valle, H. F., Eglinton, T., Rozanski, K. and Zech, M.: Coupling $\delta^{2}H$ and $\delta^{18}O$ biomarker results yields information on relative humidity and isotopic composition of precipitation - a climate transect validation study, Biogeosciences, 12, 3913–3924, doi:10.5194/bg-12-3913-2015, 2015.

Evaluation of bacterial glycerol dialkyl glycerol tetraether and ^{2}H-^{18}O biomarker proxies along a Central European topsoil transect

Johannes Hepp[1,2,*], Imke K. Schäfer[3], Verena Lanny[4], Jörg Franke[3], Marcel Bliedtner[3,a], Kazimierz Rozanski[5], Bruno Glaser[2], Michael Zech[2,6], Timothy I. Eglinton[4], Roland Zech[3,a]

[1]Chair of Geomorphology and BayCEER, University of Bayreuth, 95440 Bayreuth, Germany and
[2]Institute of Agronomy and Nutritional Sciences, Soil Biogeochemistry, Martin-Luther-University Halle-Wittenberg, 06120 Halle, Germany
[3]Institute of Geography and Oeschger Centre for Climate Change Research, University of Bern, 3012 Bern, Switzerland
[4]Department of Earth Science, ETH Zurich, 8092 Zurich, Switzerland
[5]Faculty of Physics and Applied Computer Science, AGH University of Science and Technology, 30-059 Kraków, Poland
[6]Institute of Geography, Faculty of Environmental Sciences, Technical University of Dresden, 01062 Dresden, Germany
[a]now at Institute of Geography, Chair of Physical Geography, Friedrich-Schiller University of Jena, 07743 Jena, Germany

*corresponding author (johannes-hepp@gmx.de)

Keywords

Leaf wax *n*-alkanes, hemicellulose sugars, pH, temperature, CBT, MBT', precipitation δ^2H and $\delta^{18}O$, relative humidity

Abstract

Molecular fossils, like bacterial branched glycerol dialkyl glycerol tetraethers (brGDGTs), and the stable isotopic composition of biomarkers, such as δ^2H of leaf wax-derived *n*-alkanes ($\delta^2H_{n\text{-alkane}}$) or $\delta^{18}O$ of hemicellulose-derived sugars ($\delta^{18}O_{sugar}$) are increasingly used for the reconstruction of past climate and environmental conditions. Plant-derived $\delta^2H_{n\text{-alkane}}$ and $\delta^{18}O_{sugar}$ values record the isotopic composition of plant source water ($\delta^2H_{source\text{-}water}$ and $\delta^{18}O_{source\text{-}water}$), which usually reflects mean annual precipitation ($\delta^2H_{precipiation}$ and $\delta^{18}O_{precipiation}$), modulated by evapotranspirative leaf water enrichment and biosynthetic fractionation. Accuracy and precision of respective proxies should be ideally evaluated at a regional scale. For this study, we analysed topsoils below coniferous and deciduous forests, as well as grassland soils along a Central European transect in order to investigate the variability and robustness of various proxies, and to identify effects related to vegetation. Soil pH-values derived from brGDGTs correlate reasonably well with measured soil pH-values, but systematically overestimate them (ΔpH = 0.6 ±0.6). The branched vs. isoprenoid tetraether index (BIT) can give some indication whether the pH reconstruction is reliable. Temperatures derived from brGDGTs overestimate mean annual air temperatures slightly (ΔT_{MA} = 0.5°C ±2.4). Apparent isotopic fractionation ($\varepsilon_{n\text{-alkane/precipitation}}$ and $\varepsilon_{sugar/precipitation}$) is lower for grassland sites than for forest sites due to "signal damping", i.e. grass biomarkers do not record the full evapotranspirative leaf water enrichment. Coupling $\delta^2H_{n\text{-alkane}}$ with $\delta^{18}O_{sugar}$ allows to reconstruct the stable isotopic composition of the source water more accurately than without the coupled approach ($\Delta\delta^2H$ = ~-21‰ ±22 and $\Delta\delta^{18}O$ = ~-2.9‰ ±2.8). Similarly, relative humidity during daytime and vegetation period (RH_{MDV}) can be reconstructed using the coupled isotope approach (ΔRH_{MDV} = ~-17 ±12). Especially for coniferous sites, reconstructed RH_{MDV} values as well as source water isotope composition underestimate the measured values. This can be likely explained by understory grass vegetation at the coniferous sites contributing significantly to the *n*-alkane pool but only marginally to the sugar pool in the topsoil. The large uncertainty likely reflect the fact that biosynthetic fractionation is not constant, as well as microclimate variability. Overall, GDGTs and the coupled $\delta^2H_{n\text{-alkane}}$-$\delta^{18}O_{sugar}$ approach have great potential for more quantitative paleoclimate reconstructions.

Gelöscht: /

Gelöscht: /

Gelöscht: /

1 Introduction

Information about the variability and consequences of past climate changes is a prerequisite for precise predictions regarding the present climate change. Molecular fossils, so called biomarkers, have great potential to enhance our understanding about variations of past climate and environmental changes. Lipid biomarkers in particular are increasingly used for paleoclimate and environmental reconstructions (e.g. Brincat et al., 2000; Eglinton and Eglinton, 2008; Rach et al., 2014; Romero-Viana et al., 2012; Schreuder et al., 2016). However strengths and limitations of respective proxies need to be known (Dang et al., 2016). For this, calibrations using modern reference samples are essential.

One famous and widely applied lipid biomarker group are terrestrial branched glycerol dialkyl glycerol tetraethers (brGDGTs). They are synthesized in the cell membranes of anaerobe heterotrophic soil bacteria (Oppermann et al., 2010; Weijers et al., 2010) have great potential for the reconstruction of past environmental conditions (e.g. Coffinet et al., 2017; Schreuder et al., 2016; Zech et al., 2012), although some uncertainties exist. Calibration studies suggest that the relative abundance of the individual brGDGTs varies with mean annual air temperature (T_{MA}) and soil pH (Peterse et al., 2012; Weijers et al., 2007), at least across large, global climate gradients or along pronounced altitudinal gradients (Wang et al., 2017). However, in arid regions the production of brGDGT is limited, while isoprenoidal GDGTs (iGDGTs) produced by archaea provide the dominant part of the overall soil GDGT pool (Anderson et al., 2014; Dang et al., 2016; Dirghangi et al., 2013; Wang et al., 2013; Xie et al., 2012). The ratio of brGDGTs vs. isoprenoid GDGTs (BIT) can be used as indication whether a reconstruction of T_{MA} and pH will be reliable. Moreover, Mueller-Niggemann et al. (2016) revealed an influence of the vegetation cover on the brGDGT producing soil microbes. From field experiments, it is known that vegetation type and mulching practice strongly effect soil temperature and moisture (Awe et al., 2015; Liu et al., 2014). Thus, multiple factors can be expected to influence soil microbial communities and GDGT production. So far, little is known about the variability of GDGT proxies on a regional scale, and a calibration study with small climate gradient but with different vegetation types might be useful.

Concerning paleohydrology proxies, compound specific stable hydrogen isotopes of leaf wax biomarkers, such as long chain *n*-alkanes ($\delta^2H_{n\text{-alkanes}}$) record the isotopic signal of precipitation and therefore past climate and environmental conditions (Sachse et al., 2004, 2006). However, various influencing factors are known e.g. the moisture source to leaf waxes (Pedentchouk and Zhou, 2018 and Sachse et al., 2012 for review). Next is the evapotranspiration of leaf water (Feakins and Sessions, 2010; Kahmen et al., 2013; Zech et al., 2015), which is strongly driven by relative air humidity (RH; e.g. Cernusak et al., 2016 for review). In addition, a strong precipitation signal is known to be incorporated into long chain leaf waxes (Hou et al., 2008; Rao et al., 2009; Sachse et al., 2004). In paleoclimate studies, it is often not feasible to disentangle between the evapotranspirative enrichment from the precipitation signal. Zech et al. (2013) proposed to couple $\delta^2H_{n\text{-alkane}}$ results with oxygen stable isotopes of hemicellulose-derived sugars ($\delta^{18}O_{sugar}$). Assuming constant biosynthetic fractionation factors (ε_{bio}) for the different compound classes (*n*-alkanes and hemicellulose sugars), the coupling enables the reconstruction of the isotopic composition of leaf water, RH and δ^2H and $\delta^{18}O$ of plant source water ($\approx \delta^2H$ and $\delta^{18}O$ of precipitation; Tuthorn et al., 2015). So far, a detailed evaluation of

Gelöscht: climate proxies
Gelöscht: ,
Gelöscht: Terrestrial
Gelöscht: that
Gelöscht: ,
Gelöscht: Compound
Gelöscht: all along the way
Gelöscht: from
Gelöscht: One
Gelöscht: /
Gelöscht: /

this approach on the European scale, as well as related effects concerning vegetation changes is missing.

We analysed topsoil samples under coniferous, deciduous and grassland vegetation along a Central European transect in order to estimate the variability of the biomarker proxies. More specifically, we aim to test whether:

(i) the vegetation type has an influence on the brGDGT proxies, the $\delta^2H_{n\text{-alkane}}$ and the $\delta^{18}O_{sugar}$ stable isotopic composition, as well as on reconstructed $\delta^2H_{source\text{-}water}$, $\delta^{18}O_{source\text{-}water}$ and RH.

(ii) the published brGDGT proxies used for reconstructing mean annual temperature and soil pH are sensitive enough to reflect the medium changes in temperature and soil pH along our transect.

(iii) the coupled $\delta^2H_{n\text{-alkane}}$-$\delta^{18}O_{sugar}$ approach enables a δ^2H and $\delta^{18}O$ of precipitation and RH reconstruction along the transect.

2 Material and methods

2.1 Geographical setting and sampling

In November 2012, we collected 29 topsoil samples (0-5 cm depth) from 16 locations along a transect from Southern Germany to Southern Sweden (Fig. 1A). We distinguished between sites with coniferous forest (con, n = 9), deciduous forest (dec, n = 14) and grassland (grass, n = 6) vegetation cover (for more details see Schäfer et al. (2016) and Tab. S1).

2.2 Database of instrumental climate variables and isotope composition of precipitation

Climate data was derived from close-by weather observation stations operating by the regional institutions (Deutscher Wetterdienst (DWD) for Germany, Danmarks Meteorologiske Institut (DMI) for Denmark and the Sveriges Meteorologiska och Hydrologiska Institute (SMHI) for Sweden). The DWD provides hourly data for each station (DWD Climate Data Center, 2018b), enabling not only the calculation of T_{MA}, but also of the mean annual relative air humidity (RH_{MA}), mean temperature and relative air humidity during the vegetation period (T_{MV} and RH_{MV}), and of daytime temperature and relative humidity averages over the vegetation period (T_{MDV} and RH_{MDV}). In addition, annual precipitation observations were used to derive the mean annual precipitation amount (P_{MA}; DWD Climate Data Center, 2018b). From the DMI, the respective climate variables were derived from published technical reports (Cappelen, 2002; Frich et al., 1997; Laursen et al., 1999). The SMHI provides open data from which we derived the climate variables for the Swedish sites (Swedish Meteorological and Hydrological Institute, 2018). For more details about the climate database used for calculations and comparisons, the reader is referred to Tab. S2.

For comprising German precipitation $\delta^2H/\delta^{18}O$ along the transect, we realized a regionalisation (called δ^2H_{GIPR} and $\delta^{18}O_{GIPR}$) using online available data from 34 German GNIP stations, 4 Austrian ANIP stations and the Groningen GNIP station (van Geldern et al., 2014; IAEA/WMO, 2018; Stumpp et al., 2014; Umweltbundesamt GmbH, 2018), following the approach of Schlotter (2007). However, instead of the multivariate regression procedure applied

Gelöscht: concerning possible effects
Gelöscht: to
Gelöscht: /
Gelöscht: faithfully reflects
Gelöscht: /
Gelöscht: at
Gelöscht: and
Gelöscht: /
Gelöscht: /
Gelöscht: /

by Schlotter (2007), we used a random forest approach (Hothorn et al., 2006; Strobl et al., 2007, 2008) to describe the relationship of squared latitude, latitude, longitude and altitude vs. long term weighted means of precipitation δ^2H and $\delta^{18}O$, and realized the prediction for each site (see supplementary method description for more information). For the Danish and Swedish sites, such a procedure was not possible. Hence, the annual precipitation δ^2H and $\delta^{18}O$ values were derived from the Online Isotopes in Precipitation Calculator (OIPC, version 3.1), therefore called δ^2H_{OIPC} and $\delta^{18}O_{OIPC}$ (Bowen, 2018; Bowen and Revenaugh, 2003; IAEA/WMO, 2015). The finally used $\delta^2H_{GIPR,OIPC}$ and $\delta^{18}O_{GIPR,OIPC}$ data are given in Tab. S1.

The T_{MA} along the transect ranges from 5.3 to 10.6°C, and P_{MA} ranges from 554 to 1769 mm (Fig. 1B). Precipitation $\delta^2H/\delta^{18}O$ shows moderate changes along the transect, $\delta^2H_{GIPR/OIPC}$ varies between -52 and -79‰, and $\delta^{18}O_{GIPR/OIPC}$ ranges from -7.4 to -10.9‰ (Fig. 1C).

Correlations between $\delta^{18}O_{GIPR/OIPC}$ and P_{MA}, altitude of the locations, T_{MA} are given in the supplementary material (Fig. S1 to S3), along with a $\delta^2H_{GIPR/OIPC}$ vs. $\delta^{18}O_{GIPR/OIPC}$ scatter plot (Fig. S4).

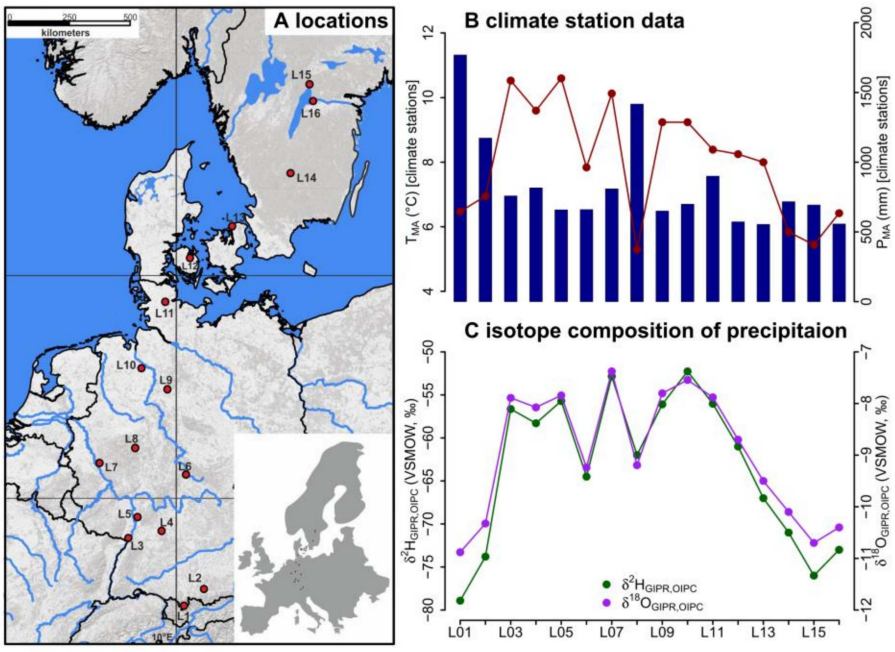

Fig. 1. (A) Sample locations (red dots, map source: US National Park Service), (B) variations of mean annual air temperature (T_{MA}, red dots and line) and mean annual precipitation (P_{MA}, blue bars) derived from close-by climate station data, and (C) hydrogen and oxygen stable isotope composition of precipitation ($\delta^2H_{GIPR/OIPC}$ and $\delta^{18}O_{GIPR/OIPC}$, respectively) as derived for the sampled transect locations (see section 2.2 GIPR δ^2H and $\delta^{18}O$ generation procedure). The reader is referred to section 2.2 (and Tab. S1 and S2) for database and reference information of data plotted in (B) and (C).

Gelöscht: /
Gelöscht: the
Gelöscht: study site
Gelöscht: s
Gelöscht: /
Gelöscht: /
Gelöscht: /
Gelöscht: /
Gelöscht: /

2.3 Soil extractions and analysis

2.3.1 GDGTs and pH

A detailed description of sample preparation for lipid analysis can be found in Schäfer et al. (2016). Briefly, 1–6 g freeze-dried and grounded soil sample was microwave extracted with 15 ml dichloromethane (DCM)/methanol (MeOH) 9:1 *(v:v)* at 100°C for 1 h. Extracts were separated over aminopropyl silica gel (Supelco, 45 µm) pipette columns. The nonpolar fraction (including *n*-alkanes) was eluted with hexane and further purified over $AgNO_3$ coated silica pipette columns (Supelco, 60-200 mesh) and zeolite (Geokleen Ltd.). The GDGT-containing fraction was eluted with DCM:MeOH 1:1 *(v:v)*, re-dissolved in hexane/isopropanol (IPA) 99:1 *(v:v)* and transferred over 0.45 µm PTFE filters into 300 µl inserts. For quantification, a known amount of a C_{46} diol standard was added after transfer. The samples were analysed at ETH Zurich using an Agilent 1260 Infinity series HPLC–atmospheric chemical pressure ionization mass spectrometer (HPLC–APCI-MS) equipped with a Grace Prevail Cyano column (150 mm × 2.1 mm; 3 µm). The GDGTs were eluted isocratically with 90% A and 10% B for 5 min and then with a linear gradient to 18% B for 34 min at 0.2 ml min^{-1}, where A=hexane and B=hexane/isopropanol (9:1, *v:v*). Injection volume was 10 µl and single ion monitoring of $[M+H]^+$ was used to detect GDGTs.

The pH of the samples was measured in the laboratory of the Soil Biogeochemistry group, Institute of Agronomy and Nutritional Sciences, Martin-Luther-University Halle-Wittenberg, using a pH meter in a 1:3 soil:water *(w/v)* mixture.

2.3.2 $\delta^2H_{n\text{-alkane}}$

The hydrogen isotopic composition of the highest concentrated *n*-alkanes (*n*-C_{25}, *n*-C_{27}, *n*-C_{29}, *n*-C_{31}, and *n*-C_{33}) was determined using a TRACE GC Ultra Gas Chromatography connected to a Delta V Plus Isotope Ratio Mass Spectrometer via a ^2H pyrolysis reactor kept at 1420 °C (GC-^2H-Py-IRMS; Thermo Scientific, Bremen, Germany) at ETH Zurich (Christoph et al., 2019). For more details about *n*-alkane quantification the reader is refereed to Schäfer et al. (2016). The compound-specific $^2H/^1H$ ratios were calibrated against an external standard with C_{15} – C_{35} homologues. External standard mixtures (A4 mix from A. Schimmelmann, University of Indiana) were run between the samples for multipoint linear normalization. The H^+_3 factor was determined on each measurement day and was constant throughout the periods of the sample batches. Samples were analysed in duplicates, and results typically agreed within 4% (average difference = 1.4%). All δ^2H values are expressed relative to the Vienna Standard Mean Ocean Water (V-SMOW).

Gelöscht: the

Formatiert: Schriftart: Kursiv

2.3.3 $\delta^{18}O_{sugar}$

Hemicellulose sugars were extracted and purified using a slightly modified standard procedure (Amelung et al., 1996; Guggenberger et al., 1994; Zech and Glaser, 2009). Briefly, myoinositol was added to the samples prior to extraction as first internal standard. The sugars were released hydrolytically using 4M trifluoroacetic acid for 4 h at 105°C, cleaned over glass fiber filters and further purified using XAD and Dowex columns. Before derivatization with methylboronic acid (Knapp, 1979), the samples were frozen, freeze-dried, and 3-O-methylglucose in dry pyridine

was added as second internal standard. Compound-specific hemicellulose sugar ^{18}O measurements were performed in the laboratory of the Soil Biogeochemistry group, Institute of Agronomy and Nutritional Sciences, Martin-Luther-University Halle-Wittenberg, using GC-^{18}O-Py-IRMS (all devices from Thermo Fisher Scientific, Bremen, Germany). Standard deviations of the triplicate measurements were 1.4‰ (over 29 investigated samples) for arabinose and xylose, respectively. We focus on these two hemicellulose-derived neutral sugars arabinose and xylose as they strongly predominate over fucose in terrestrial plants, soils and sediments (Hepp et al., 2016 and references therein). Rhamnose concentrations were too low to obtain reliable $\delta^{18}O$ results. All $\delta^{18}O$ values are expressed relative to the Vienna Standard Mean Ocean Water (V-SMOW).

2.4 Theory and Calculations

2.4.1 Calculations used for the GDGT-based reconstructions

The branched and isoprenoid tetraether (BIT) index is calculated according to Hopmans et al. (2004), for structures see Fig. S5:

$$BIT = \frac{Ia+IIa+IIIa}{Ia+IIa+IIIa+crenarchaeol}. \quad (1)$$

The cyclopentane moiety number of brGDGTs correlates negatively with soil pH (Weijers et al., 2007), which led to the development of the cyclization of branched tetraethers (CBT) ratio. CBT and the CBT based pH (pH_{CBT}) were calculated according to Peterse et al. (2012):

$$CBT = -\log\frac{Ib+IIb}{Ia+IIa}, \quad (2)$$

$$pH_{CBT} = 7.9 - 1.97 \times CBT. \quad (3)$$

The number of methyl groups in brGDGTs correlates negatively with T_{MA} and soil pH (Peterse et al., 2012; Weijers et al., 2007). Thus, the ratio of the methylation of branched tetraethers (MBT) ratio and the CBT ratio can be used to reconstruct T_{MA}. We use the equation given by Peterse et al. (2012):

$$MBT' = \frac{Ia+Ib+Ic}{Ia+Ib+Ic+IIa+IIb+IIc+IIIa}, \quad (4)$$

$$T_{MA} = 0.81 - 5.67 \times CBT + 31.0 \times MBT'. \quad (5)$$

2.4.2 Calculations and concepts used for the coupled δ^2H-$\delta^{18}O$ approach

The apparent fractionation is calculated according to Cernusak et al. (2016):

$$\varepsilon_{n\text{-alkane/precipitation}} = \left(\frac{\delta^2H_{n\text{-alkane}} - \delta^2H_{GIPR,OIPC}}{1+\delta^2H_{GIPR,OIPC}/1000}\right), \quad (6)$$

$$\varepsilon_{sugar/precipitation} = \left(\frac{\delta^{18}O_{sugar} - \delta^{18}O_{GIPR,OIPC}}{1+\delta^{18}O_{GIPR,OIPC}/1000}\right). \quad (7)$$

The isotopic composition of leaf water ($\delta^2H_{leaf\text{-}water}$ and $\delta^{18}O_{leaf\text{-}water}$) can be calculated using ε_{bio} for $\delta^2H_{n\text{-alkane}}$ (-160‰, Sachse et al., 2012; Sessions et al., 1999) and $\delta^{18}O_{sugar}$ (+27‰, Cernusak et al., 2003; Schmidt et al., 2001):

$$\delta^2H_{leaf\text{-}water} = \left(\frac{1000+\delta^2H_{n\text{-alkane}}}{1000+\varepsilon_{bio}\ (n\text{-alkane})}\right) \times 10^3 - 1000, \quad (8)$$

Gelöscht: /

Formatiert: Schriftart: Kursiv

Gelöscht: /

Formatiert: Schriftart: Kursiv

Gelöscht: /

Gelöscht: /

Gelöscht: /$\delta^{18}O_{leaf}$

Gelöscht:

$$\delta^{18}O_{leaf\text{-}water} = \left(\frac{1000+\delta^{18}O_{sugar}}{1000+\varepsilon_{bio\ (sugar)}}\right) \times 10^3 - 1000. \quad (9)$$

Zech et al. (2013) introduced the conceptual model for the coupled $\delta^2H_{n\text{-alkane}}$-$\delta^{18}O_{sugar}$ approach in detail. Briefly, the coupled approach is based on the following assumptions (illustrated in Fig. 8): (i) The isotopic composition of precipitation, which is set to be equal to the plant source water, typically plots along the global meteoric water line (GMWL; $\delta^2H = 8 \times \delta^{18}O + 10$) in a $\delta^{18}O$ vs. δ^2H space (Craig, 1961); (ii) Source water uptake by plants does not lead to any fractionation (e.g. Dawson et al., 2002), and significant evaporation of soil water can be excluded; (iii) Evapotranspiration leads to enrichment of the remaining leaf water along the local evaporation line (LEL; Allison et al., 1985; Bariac et al., 1994; Walker and Brunel, 1990), compared to the source water taken up by the plant; (iv) The biosynthetic fractionation is assumed to be constant. In addition, isotopic equilibrium between plant source water (~ weighted mean annual precipitation) and the local atmospheric water vapour is assumed. Further assumption concerns the isotope steady-state in the evaporating leaf water reservoir. The coupled approach allows for reconstructing the isotopic composition of plant source water ($\delta^2H_{source\text{-}water}$ and $\delta^{18}O_{source\text{-}water}$) from the reconstructed leaf water, by calculating the intercepts of the LELs with the GMWL (Zech et al., 2013). The slope of the LEL (S_{LEL}) can be assessed by the following equation (Gat, 1971):

$$S_{LEL} = \frac{\varepsilon_2^* + C_k^2}{\varepsilon_{18}^* + C_k^{18}}, \quad (10)$$

where ε^* are equilibrium isotope fractionation factors and C_k are kinetic fractionation factors. The latter equals to 25.1‰ and 28.5‰, for C_k^2 and C_k^{18}, respectively (Merlivat, 1978). The equilibrium fractionation factors can be derived from empirical equations (Horita and Wesolowski, 1994) by using T_{MDV} values. For two Danish sites T_{MDV} are not available, instead T_{MV} is used here (section 2.2 and Tab. S2).

In a $\delta^{18}O$-δ^2H diagram, the distance of the leaf water from the GMWL define the deuterium-excess of leaf water ($d_{leaf\text{-}water} = \delta^2H_{leaf\text{-}water} - 8 \times \delta^{18}O_{leaf\text{-}water}$, according Dansgaard, (1964); Fig. 8). To convert $d_{leaf\text{-}water}$ into mean RH during daytime and vegetation period (RH_{MDV}), a simplified Craig-Gordon model can be applied (Zech et al., 2013):

$$RH = 1 - \frac{\Delta d}{\varepsilon_2^* - 8 \times \varepsilon_{18}^* + C_k^2 - 8 \times C_k^{18}}, \quad (11)$$

where Δd is the difference in $d_{leaf\text{-}water}$ and the deuterium-excess of source water ($d_{source\text{-}water}$).

2.5 Statistics

In the statistical analysis we checked sample distributions for normality (Shapiro and Wilk, 1965) and for equal variance (Levene, 1960). If normality and equal variances are given, we perform an Analysis of Variance (ANOVA). If that is not the case, we conduct the non-parametric Kruskal-Wallis Test. ANOVA or Kruskal-Wallis are used to find significant differences (a=0.05) between the vegetation types (deciduous, conifer and grass).

In order to describe the relation along a 1:1 line, the coefficient of correlation (R^2) was calculated as $R^2 = 1 - \sum (\text{modeled} - \text{measured})^2 / \sum(\text{measured} - \text{measured mean})^2$. The small r^2 is taken as coefficient of correlation of a linear regression between a dependent (y) and

Gelöscht:

Gelöscht: /

explanatory variable(s). The root mean square error (RMSE) of the relationships was calculated as RMSE = $\sqrt{\left(\frac{1}{n} \cdot \sum(\text{modeled - measured})^2\right)}$. All data plotting and statistical analysis was realized in R (version 3.2.2; R Core Team, 2015).

3 Results and Discussion

3.1 GDGT concentrations

GDGT Ia has the highest concentration under all vegetation types, followed by GDGT IIa and GDGT IIIa (Fig. 2). GDGT Ib, IIb and Ic occur in minor, GDGT IIc and IIIb only in trace amounts. GDGT IIIc was below the detection limit in most of the samples (Tab. S3). Although other studies document an influence of the vegetation cover on soil temperature and soil water content, which control the microbial community composition in soils (Awe et al., 2015; Liu et al., 2014; Mueller-Niggemann et al., 2016), we find no statistically different pattern of the individual brGDGTs.

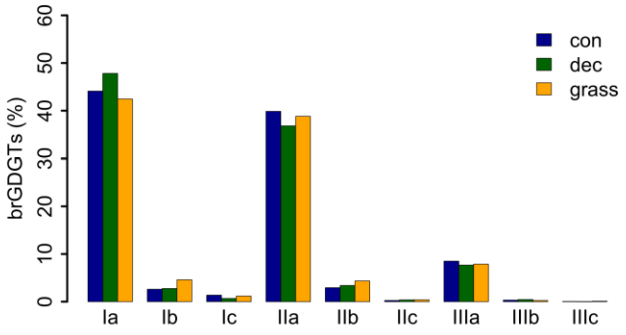

Fig. 2. Mean concentrations of individual brGDGTs as percentage of all brGDGTs for the three investigated types. Abbreviations: con = coniferous forest sites (n=9); dec = deciduous forest sites (n=14); grass = grassland sites (n=6).

Total concentrations of brGDGTs range from 0.32 to 9.17 µg/g dry weight and tend to be highest for the coniferous samples and lowest for the grasses (Fig. 3A, Tab. S3). Bulk brGDGT concentrations lie within the range of other studies examining soils of mid latitude regions (Huguet et al., 2010b, 2010a; Weijers et al., 2011). Similar concentrations in coniferous and deciduous samples imply that brGDGT production does not strongly vary in soils below different forest types. The grass samples show lower brGDGT concentrations compared to the forest samples, but this is probably mainly due to ploughing of the grass sites in former times and hence admixing of mineral subsoil material. The differences in brGDGT concentrations are not significant (p-value = 0.06).

Gelöscht: s

Gelöscht: Anyhow, t

3.2 BIT index

Most of the samples have a BIT index higher than 0.9 (Fig 3B and Tab. S3). The BIT-values are typical for soils in humid and temperate climate regions (Weijers et al., 2006). However,

outliers exist. The most likely source of iGDGTs in soils are Thaumarchaeota, i.e. aerobe ammonia oxidizing archaea producing Crenarchaeol and its regioisomer (Schouten et al., 2013 and references therein), precipitation amounts drop below 700-800 mm (Dang et al., 2016; Dirghangi et al., 2013). The P_{MA} data of our sampling sites mostly show precipitation > 550 mm (Fig. 1B), but one has to be aware that this data is based on the climate station nearest to the respective sampling locations and microclimate effects, such as sunlight exposure, canopy cover or exposition might have a pronounced influence on the brGDGT vs. iGDGT distribution. Mueller-Niggemann et al. (2016) found higher BIT indices in upland soils compared to paddy soils and stated that the management type also influences BIT values in soils. Along our transect, grass sites tend to have slightly lower BIT-values than forest sites, probably due to the absence of a litter layer and hence, no isolation mechanism preventing evaporation of soil water. Differences between vegetation types are not significant (p-value = 0.32).

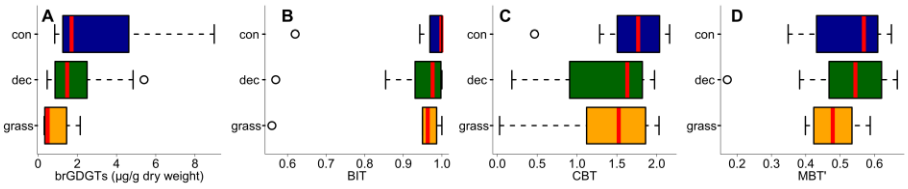

Fig. 3. (A) Total concentrations of brGDGTs in µg g^{-1} dry weight, as well as (B) BIT, (C) CBT and (D) MBT'. Abbreviations: con = coniferous forest sites (n=9); dec = deciduous forest sites (n=14); grass = grassland sites (n=6). Box plots show median (red line), interquartile range (IQR) with upper (75%) and lower (25%) quartiles, lowest whisker still within 1.5IQR of lower quartile, and highest whisker still within 1.5IQR of upper quartile, dots mark outliers.

3.3 CBT-derived pH

The CBT ratio shows a pronounced variation independent of vegetation type with values between 0.03 and 2.16 (Fig 3C). The coniferous samples tend to be highest, but the differences between vegetation types are not significant (p-value = 0.48). The CBT index can be related to pH in acidic and/or humid soils (e.g. Dirghangi et al., 2013; Mueller-Niggemann et al., 2016; Peterse et al., 2012; Weijers et al., 2007) but might be an indicator of soil water content and hence, precipitation in more arid and alkaline soils (e.g. Dang et al., 2016). There is a pronounced correlation between CBT and soil pH (Fig. 4), which is in good agreement with other studies from mid latitude regions where precipitation is relatively high (Anderson et al., 2014 and references therein). Moreover, the CBT to pH relationship in terms of slope and intersect in our dataset (CBT = -0.47 × pH + 3.5, r^2 = 0.7, p-value < 0.0001, n = 29) is well comparable to the correlation described for the global calibration dataset of Peterse et al. (2012) (CBT = -0.36 × pH + 3.1, r^2 = 0.7, p-value < 0.0001, n = 176).

However, there are some outliers in the CBT-pH correlation, which need a further examination (see locations grass L04, dec L10 and dec L12 as marked in Figs. 4 and 5). The outliers show lower BIT indices (< 0.85, Tab. S3). Even though the data from the nearest climate station suggest no abnormal P_{MA}. Local effects such as differences in the amount of sunlight exposure, nutrient availability for brGDGT producing organisms or, most likely soil water content might influence the brGDGT production at these locations (Anderson et al., 2014; Dang et al., 2016).

Gelöscht: Anyhow,

Gelöscht: d

A lower BIT index as well as a lower CBT occur when soil water content decreases (Dang et al., 2016; Sun et al., 2016) or when aeration is high and less anoxic microhabitats for GDGT producing microbes exist (e.g. Dirghangi et al., 2013).

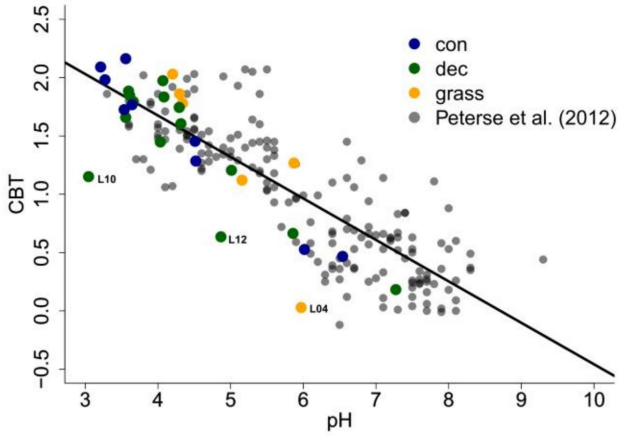

Fig. 4. CBT to pH relationship in our dataset in comparison to the global calibration dataset from Peterse et al. (2012) (CBT = -0.36 × pH + 3.1, r^2 = 0.7, p-value < 0.0001, n = 176, black line). Abbreviations: con = coniferous forest sites (n=9); dec = deciduous forest sites (n=14); grass = grassland sites (n=6).

As the CBT and pH are similarly correlated in our dataset and the global dataset of Peterse et al. (2012), the CBT-derived pH correlated well with the actual pH (Fig. 5A; R^2 = 0.3). Expressed as ΔpH (CBT-derived pH - measured pH), there is a tendency that the GDGTs result in an overestimation of the real pH for the forest sites (Fig. B). Yet a Kruskal-Wallis test shows no statistically significant difference between the vegetation types, with a p-value of 0.13. The overall ΔpH of 0.6 ±0.6 shows that the reconstruction of soil pH using brGDGTs works well along this transect.

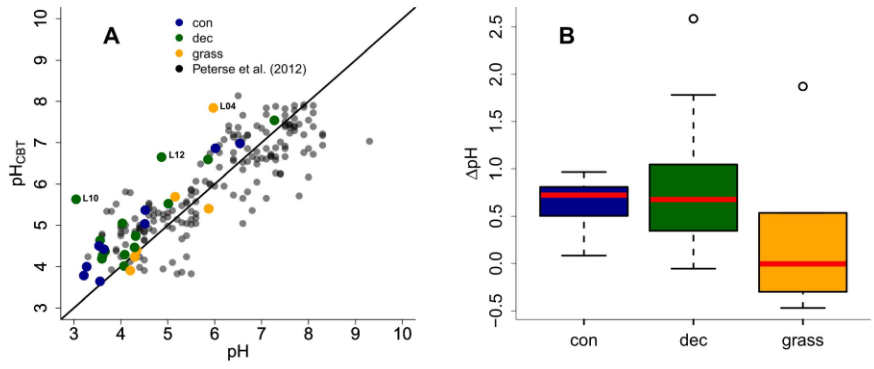

Fig. 5. (A) Correlation between measured pH and reconstructed soil pH (pH_{CBT}) from our transect data in comparison to the global calibration dataset from Peterse et al. (2012) ($R^2 = 0.7$, RMSE = 0.75, n = 176). Black line indicates the 1:1 relationship. (B) Boxplots of ΔpH (refers to pH_{CBT}-pH). Box plots show median (red line), interquartile range (IQR) with upper (75%) and lower (25%) quartiles, lowest whisker still within 1.5IQR of lower quartile, and highest whisker still within 1.5IQR of upper quartile, dots mark outliers. Abbreviations: con = coniferous forest sites (n=9); dec = deciduous forest sites (n=14); grass = grassland sites (n=6).

3.4 MBT'-CBT-derived T_{MA} reconstructions

The MBT' shows high variability with values ranging from 0.17 to 0.67 no statistical differences between vegetation types (p-value = 0.54; Fig. 3D, Tab. S3). When comparing reconstructed (MBT'-CBT-derived) T_{MA} with climate station T_{MA}, the data plot close to the 1:1 line, and fit well into the global dataset of Peterse et al. (2012) (Fig. 6A). The ΔT_{MA} reveal an overall offset of 0.5°C ±2.4 and there is no statistically difference between vegetation types (Fig. 6B). The standard deviation in ΔT_{MA} of ±2.4 is well in line with the RMSE of 5.0 for the global calibration dataset (Peterse et al., 2012).

Gelöscht: 7A

Gelöscht: 7B

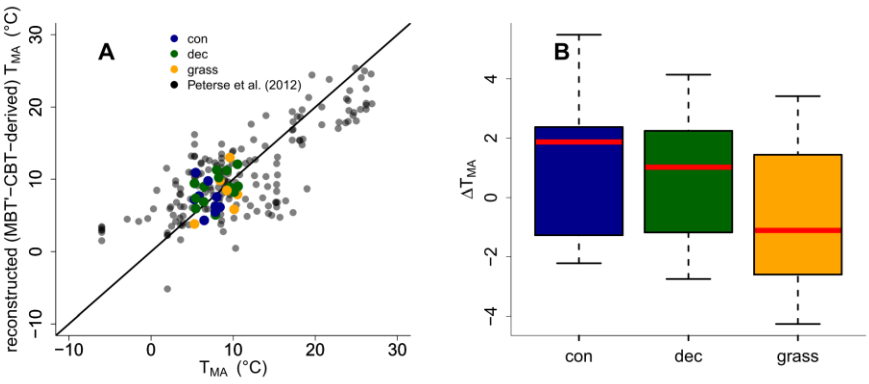

Fig. 6. (A) Correlation between climate station T_{MA} and reconstructed (MBT'-CBT-derived) T_{MA}. For comparison, the global calibration dataset from Peterse et al. (2012) is shown. The black line indicates the 1:1 relationship. (B) Boxplots of ΔT_{MA} (refers to reconstructed T_{MA}-T_{MA} from climate stations) in the different vegetation types from our transect study. Box plots show median (red line), interquartile range (IQR) with upper (75%) and lower (25%) quartiles, lowest whisker still within 1.5IQR of lower quartile, and highest whisker still within 1.5IQR of upper quartile, dots mark outliers. Abbreviations: con = coniferous forest sites (n=9); dec = deciduous forest sites (n=14); grass = grassland sites (n=6).

3.5 Potential impact of the used liquid chromatography method on pH and T_{MA} reconstructions

The GDGT data presented in this study are not acquired on the up-to-date method (e.g. compare De Jonge et al., 2014 vs. Zech et al., 2012c). De Jonge et al. (2014) presented a new liquid chromatography method which enables the separation for the brGDGTs with m/z 1036, 1034

and 1032, 1050, 1048 and 1046 into 6-methyl and 5-methyl stereoisomers. The old method did not allow such a separation (Zech et al., 2012c), thus in the calibration often the sum of 6 and 5-methlyted brGDGTs was used (see and compare De Jonge et al., 2014 vs. Peterse et al., 2012). This introduce scatter to the MBT'-CBT-based T_{MA} reconstructions and can cause a correlation between pH and MBT' (for more details see De Jonge et al., 2014). De Jonge et al. (2014) moreover show that the 6-methyl brGDGTs are ubiquitous abundant in soils from all over the world, based on reanalysing the dataset of Peterse et al. (2012). However, they also compare reconstructed T_{MA} values based MBT'-CBT calibration (Peterse et al., 2012) and their new developed T_{MA} calibration and state that they plot around a 1:1 line. They furthermore state, that especially for arid areas larger deviations can be expected. Finally, they conclude that the use of the new developed calibrations will improve the T_{MA} and pH reconstructions for areas with arid climate conditions. Because our study transect spans form southern Germany to southern Sweden, representing temperate and humid climate conditions, we argue that the usage of the older liquid chromatorgraphy method do not introduce a systematic error in our T_{MA} and pH reconstructions. Still, a higher variability/scatter could be associated with the calibration of Peterse et al. (2012) and therefore also present in our T_{MA} and pH reconstructions.

3.6 Apparent fractionation of δ^2H and $\delta^{18}O$ in the different vegetation types

Gelöscht: 5

The δ^2H values could be obtained for *n*-alkanes C_{27}, C_{29} and C_{31} in all samples and additionally at two locations for *n*-C_{25} and *n*-C_{33} at six other locations. The $\delta^2H_{n\text{-alkane}}$ values, calculated as mean of *n*-C_{25} to *n*-C_{31} δ^2H, ranges from -156 to -216‰. Pooled standard deviations show an overall average of 3.6‰. The $\delta^{18}O_{sugar}$ values, calculated as the area weighted means for arabinose and xylose, ranges from 27.7 to 39.4‰. The average weighted mean standard deviation is 1.4‰. The compound-specific isotope data is summarized along with the calculations in Tab. S4.

Apparent fractionation ($\varepsilon_{n\text{-alkane/precipitation}}$) is on the order of -120 to -150‰, i.e. a bit less than the biosynthetic fraction of -160‰. This implies that evapotranspirative enrichment is ~ 10 to 40‰ (Fig. 7A). $\varepsilon_{n\text{-alkane/precipitation}}$ is lower for grass sites compared to the forest sites. Differences are significant between deciduous and grass sites (p-value = 0.005). This finding supports the results of other studies (Kahmen et al., 2013; Liu and Yang, 2008; McInerney et al., 2011), and can be named "signal damping". Grasses do not only incorporate the evaporatively-enriched leaf water only but also unenriched xylem water in the growth and differentiation zone of grasses (Gamarra et al., 2016; Liu et al., 2017).

Gelöscht: leaf

The grass-derived hemicellulose sugar biomarkers do not fully record the evapotranspirative enrichment of the leaf water, either, as indicated by lower apparent fractionation ($\varepsilon_{sugar/precipitation}$) in Fig. 7B. The differences are significant between forest and grass sites (p-value < 0.005). This is in agreement with a study on cellulose extracted from grass blades (Helliker and Ehleringer, 2002), and again, the "signal damping" can be explained with incorporation of enriched leaf water and non-enriched stem water.

Based on the comparison of evapotranspirative enrichment between forest and grass sites, the "signal damping" can be quantified to be ~ 31% for the hemicellulose sugars, and ~ 49% for the *n*-alkanes. This is in agreement with other studies that reported a loss of 22% of the leaf

water enrichment for hemicellulose sugars (Helliker and Ehleringer, 2002) and 39 to 62% loss of the leaf water enrichment for *n*-alkanes (Gamarra et al., 2016).

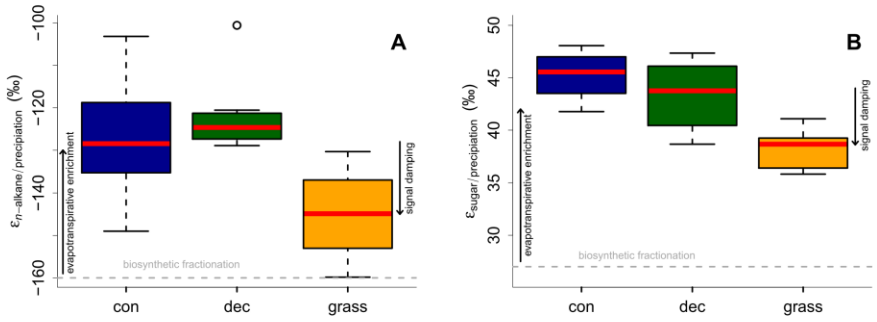

Fig. 7. Apparent fractionation (A) $\varepsilon_{n\text{-alkane/precipitation}}$ and (B) $\varepsilon_{\text{sugar/precipitation}}$. Biosynthetic fractionation factors according to section 2.4.2. Box plots show median (red line), interquartile range (IQR) with upper (75%) and lower (25%) quartiles, lowest whisker still within 1.5IQR of lower quartile, and highest whisker still within 1.5IQR of upper quartile, dots mark outliers. Abbreviations: con = coniferous forest sites (n=9); dec = deciduous forest sites (n=11 and 14 for *n*-alkanes and sugars, respectively); grass = grassland sites (n=4 and 6 for *n*-alkanes and sugars, respectively). The figure conceptually illustrates the effect of biosynthetic fractionation and evapotranspirative enrichment as well as "signal damping".

3.7 $\delta^2H_{source\text{-}water}$ and $\delta^{18}O_{source\text{-}water}$ reconstructions

The δ^2H versus $\delta^{18}O$ diagram shown in Fig. 8 graphically illustrates the reconstruction of $\delta^2H_{leaf\text{-}water}$ and $\delta^{18}O_{leaf\text{-}water}$ (colored dots) from $\delta^2H_{n\text{-}alkane}$ and $\delta^{18}O_{sugar}$ (crosses), as well as the reconstruction of $\delta^2H_{source\text{-}water}$ and $\delta^{18}O_{source\text{-}water}$ (black dots). For reconstructing $\delta^2H_{source\text{-}water}$ and $\delta^{18}O_{source\text{-}water}$, LELs with an average slope of 2.8 ±0.1 (Eq. 10) can be generated through every leaf water point and the intercepts of these LELs with the GMWL.

Gelöscht: 6
Gelöscht: /
Gelöscht: /
Gelöscht: /
Gelöscht: /
Gelöscht: /

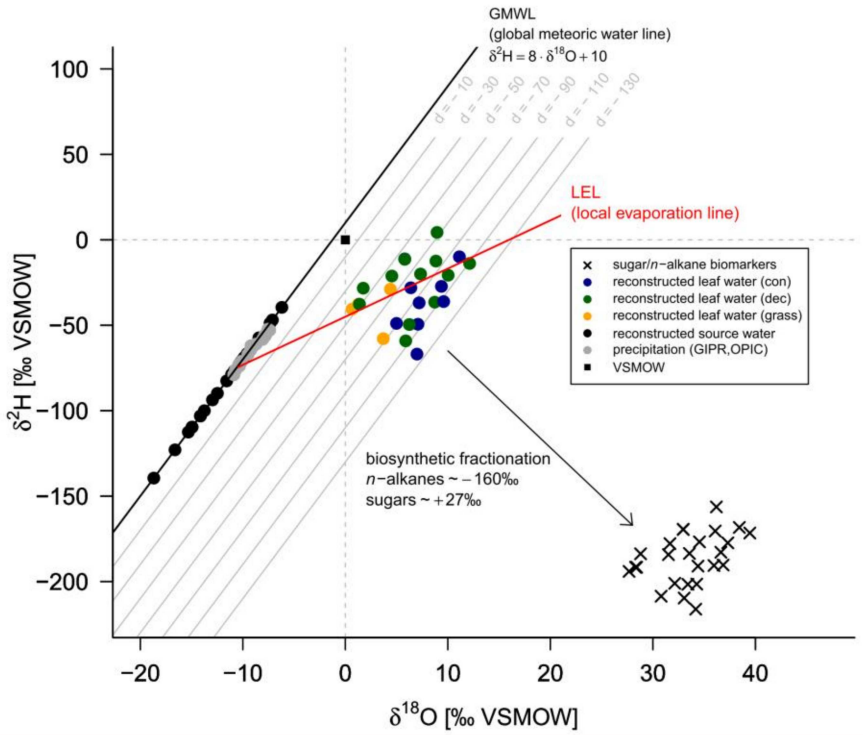

Fig. 8. δ^2H vs. $\delta^{18}O$ diagram illustrating the coupled $\delta^2H_{n\text{-alkane}}$-$\delta^{18}O_{sugar}$ approach: measured $\delta^2H_{n\text{-alkane}}$ and $\delta^{18}O_{sugar}$ values, reconstructed $\delta^2H_{leaf\text{-}water}$ and $\delta^{18}O_{leaf\text{-}water}$ (according Eqs. 8 and 9) and reconstructed $\delta^2H_{source\text{-}water}$ and $\delta^{18}O_{source\text{-}water}$ in comparison to GIPR and OIPC-based $\delta^2H_{precipitation}$ and $\delta^{18}O_{precipitation}$. Abbreviations: con = coniferous forest sites (n=9); dec = deciduous forest sites (n=11); grass = grassland sites (n=4).

The reconstructed $\delta^2H_{source\text{-}water}$ and $\delta^{18}O_{source\text{-}water}$ results can be compared with the $\delta^2H_{GIPR,OIPC}$ and $\delta^{18}O_{GIPR,OIPC}$ data (Fig. 9). This comparison reveals that the coupled $\delta^2H_{n\text{-alkane}}$-$\delta^{18}O_{sugar}$ approach yields more accurate $\delta^2H_{source\text{-}water}$ and $\delta^{18}O_{source\text{-}water}$ compared to single $\delta^2H_{n\text{-alkane}}$ approaches. However, the range of the reconstructed $\delta^2H_{source\text{-}water}$ and $\delta^{18}O_{source\text{-}water}$ values is clearly larger than in $\delta^2H_{GIPR,OIPC}$ and $\delta^{18}O_{GIPR,OIPC}$ values. δ^2H is systematically underestimated by ~ 21‰ ±22 (Fig. 9B) and $\delta^{18}O$ by ~ 2.9‰ ±2.8 (Fig. 9D). The type of vegetation seems to be not particularly relevant (p-value = 0.18 for $\Delta\delta^2H$ and p-value = 0.34 for $\Delta\delta^{18}O$). Nevertheless, the systematic offsets tend to be lowest for the decidous sites ($\Delta\delta^2H$ and $\Delta\delta^{18}O$ is closer to zero with ~-5‰ ±15 and ~-1.1‰ ±2.1), followed by grass sites (~-14‰ ±20 and ~-2.1‰ ±2.6). In comparison, the coniferous sites show the largest offsets (~-23‰ ±26 for $\Delta\delta^2H$ ~-3.0‰ ±3.3 for $\Delta\delta^{18}O$). Differences are, however, not statistically significant. The systematic offset and the large variability might have more specific reasons, and we suggest that this is related to the type of vegetation. Deciduous trees produce lots of leaf waxes and sugars (e.g.

Gelöscht: and
Gelöscht: ,
Gelöscht: /
Gelöscht: /
Gelöscht: /
Gelöscht: /
Gelöscht: /
Gelöscht: /
Gelöscht: /
Gelöscht: results than hitherto applied
Gelöscht: single isotope
Gelöscht: /
Gelöscht: /
Gelöscht: /
Gelöscht: /Δ

Prietzel et al., 2013; Zech et al., 2012a), and all biomarkers reflect and record the evapotranspirative enrichment of the leaf water (e.g. Kahmen et al., 2013; Tuthorn et al., 2014). However, coniferous trees produce quite low amounts of *n*-alkanes (Diefendorf and Freimuth, 2016; Zech et al., 2012a), while sugar concentrations are as high as in other vascular plants (e.g. Hepp et al., 2016; Prietzel et al., 2013). For the coniferous soil samples this means that the *n*-alkanes stem most likely from the understory whereas the sugars originate from grasses and coniferous needles. When the understory is dominated by grass species then the *n*-alkane biomarkers do not record the full leaf water enrichment signal, whereas the sugars from the needles do. The reconstructed leaf water for the coniferous sites is therefore too negative concerning δ^2H, and reconstructed $\delta^2H_{source\text{-}water}$ and $\delta^{18}O_{source\text{-}water}$ values thus also become too negative (Fig. 8). Concerning the grass sites the following explanation can be found. Correcting for "signal damping" makes the reconstructed leaf water points more positive and shifts them in Fig. 8 up and right. As the "signal damping" is stronger for δ^2H than for $\delta^{18}O$ the corrected leaf water points would now above the uncorrected ones. The corrected leaf water points leads to more positive reconstructed $\delta^2H_{source\text{-}water}$ and $\delta^{18}O_{source\text{-}water}$ values for the grass sites. However, Gao et al. (2014) and Liu et al. (2016) showed that the ε_{bio} of monocotyledon plants could larger than those of dicotyledonous once. This would therefore course a more negative apparent fractionation factor for grasses compared to trees. We observe that the apparent fractionation is indeed more negative for the grass sites compared to the forest sites. The effects of "signal damping" vs. variable ε_{bio} along with vegetation types are indistinguishable here. As an outlook for a future study, we therefore strongly recommend a comparison between the here measured $\delta^2H_{n\text{-alkane}}$ values with modelled once using a new available model approach from Konecky et al. (2019), which could provide insights if such vegetation effects on ε_{bio} of ^2H in *n*-alkanes are describable.

Vegetation type specific rooting depths could partly cause the overall high variability in reconstructed $\delta^2H_{source\text{-}water}$ and $\delta^{18}O_{source\text{-}water}$. Deep rooting species most likely use the water from deeper soil horizons and/or shallow ground water, which is equal to the (weighted) mean annual precipitation (e.g. Herrmann et al., 1987). Shallow rooting plants take up water from upper soil horizons, which is influenced by seasonal variations in $\delta^2H_{precipiation}$ and $\delta^{18}O_{precipiation}$ and by soil water enrichment (Dubbert et al., 2013). Thus, the overall assumption that the source water of the plants reflects the local (weighted) mean precipitation might be not fully valid for all sites. Moreover, a partly contribution of root-derived rather than leaf-derived sugar biomarkers in our topsoil samples is very likely. This does, by contrast, not apply for *n*-alkanes, which are hardly produced in roots (Zech et al., 2012b and the discussion therein).

Gelöscht: (e.g. Cernusak et al., 2016; Tuthorn et al., 2014)

Gelöscht: The coupled approach and the leaf water reconstruction based on the *n*-alkane and sugar biomarkers thus works well.

Gelöscht: /

Gelöscht: are

Gelöscht: /

Gelöscht: /

Gelöscht: /

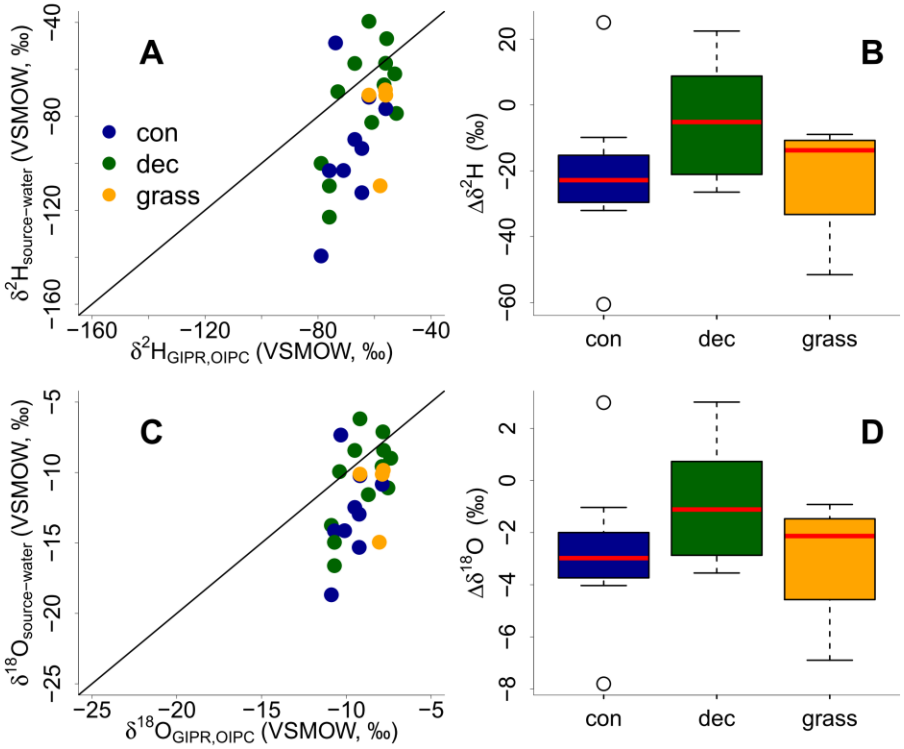

Fig. 9. Correlation of reconstructed $\delta^2H_{source-water}$ and $\delta^{18}O_{source-water}$ vs. precipitation $\delta^2H_{GIPR,OIPC}$ and $\delta^{18}O_{GIPR,OIPC}$ (A and C). Black lines indicate 1:1 relationship. Differences between reconstructed source water and precipitation ($\Delta\delta^2H,\delta^{18}O$ = $\delta^2H_{source-water},\delta^{18}O_{source-water}$ - $\delta^2H_{GIPR,OIPC},\delta^{18}O_{GIPR,OIPC}$) for the three different vegetation types (B and D). Box plots show median (red line), interquartile range (IQR) with upper (75%) and lower (25%) quartiles, lowest whisker still within 1.5IQR of lower quartile, and highest whisker still within 1.5IQR of upper quartile. Abbreviations: con = coniferous forest sites (n=9); dec = deciduous forest sites (n=11); grass = grassland sites (n=4).

Moreover, the high variability within the vegetation types could be caused by variability in ε_{bio} of ^2H in *n*-alkanes, as well as ^{18}O in sugars. There is an ongoing discussion about the correct ε_{bio} for ^{18}O in hemicellulose sugars (Sternberg, 2014 vs. Zech et al., 2014), and ε_{bio} is probably not constant over all vegetation types. This translates into errors concerning leaf water reconstruction and thus for reconstructing $\delta^2H_{source-water}$ and $\delta^{18}O_{source-water}$ values (Eq. 9 and Fig. 8). Likewise, the ε_{bio} values reported in the literature for ^2H of *n*-alkanes can be off from -160‰ by tens of permille (Feakins and Sessions, 2010; Tipple et al., 2015; Feakins et al., 2016; Freimuth et al., 2017). The degree to which hydrogen originates from NADPH rather than leaf water is important, because NADPH is more negative (Schmidt et al., 2003). The wide range in biosynthetic ^2H fractionation factors, which can be even larger, is therefore also related to the carbon and energy metabolism state of plants (Cormier et al., 2018).

Gelöscht: /
Gelöscht: /
Gelöscht: /
Gelöscht: /
Gelöscht: /
Gelöscht: /
Gelöscht: /
Gelöscht: /

3.8 RH reconstruction

Reconstructed RH_{MDV} ranges from 34 to 74%, while RH_{MDV} from climate station data range from 61 to 78% (Fig. 10A). Biomarker-based values thus systematically underestimate the station data (ΔRH_{MDV} = -17% ±12). Yet the offsets are much less for deciduous tree and grass sites (ΔRH_{MDV} = -10% ±12 and -7% ±9, respectively; Fig. 10B). The offsets for the coniferous sites are -30% ±11, and significantly larger than for the deciduous and grass sites (p-values < 0.05).

Too low reconstructed RH_{MDV} values for the coniferous sites make sense in view of the previously discussed option that soils contain *n*-alkanes from the understory (which is dominated by grass species), while sugars stem from needles and grasses. As explained earlier already, the "signal damping" leads to too negative reconstructed $\delta^2H_{leaf\text{-}water}$ (whereas $\delta^{18}O$ is affected less by the "signal damping"), and too negative $\delta^2H_{leaf\text{-}water}$ translates into overestimated d-excess and underestimated RH values. In Fig. 8, a correction for this require moving the coniferous leaf water data points upwards towards more positive δ^2H values, thus the distance between the leaf water and the source water is reduced. It should be noted that also here variable ε_{bio} along with vegetation types could not be distinguished from "signal damping" effects.

The underestimation of RH for the deciduous and grass sites could be partly associated with the use of the GMWL as baseline for the coupled $\delta^2H_{n\text{-}alkane}$-$\delta^{18}O_{sugar}$ approach. The deuterium-excess of the LMWLs is generally lower than the +10‰ of the GMWL, while the slopes of the LMWLs are well comparable to the GMWL (Stumpp et al., 2014). In addition, if soil water evaporation occurred before water uptake by the plants, this would lead to an underestimation of biomarker-based RH_{MDV} values. It can be furthermore assumed that plant metabolism is highest during times with direct sunshine and high irradiation, i.e. during noon at sunny days. The relevant RH could therefore be lower than the climate station-derived RH_{MDV}. Indeed, already climate station RH_{MDV} is considerable lower than RH_{MA} and RH_{MV} (Tab. S1).

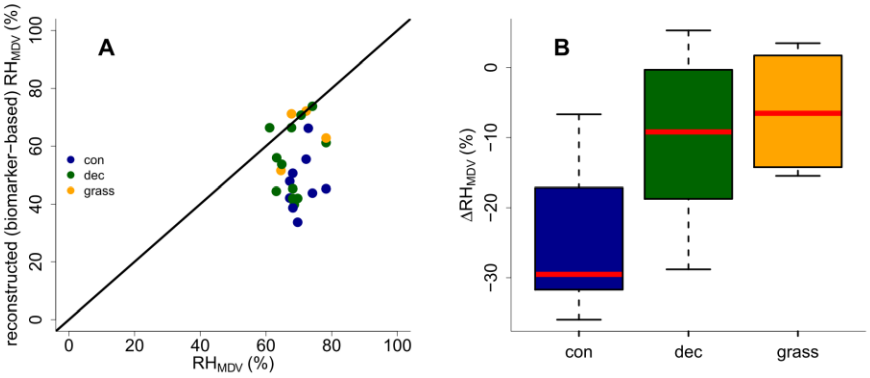

Fig. 10. (A) Comparison of reconstructed (biomarker-based) RH_{MDV} values and climate station RH_{MDV} data. The black line indicates the 1:1 relationship. (B) Differences between reconstructed and climate station RH_{MDV} values (ΔRH_{MDV} = reconstructed – climate station RH_{MDV}) for the three different vegetation types along the transect. Abbreviations: con = coniferous forest sites (n=9); dec = deciduous forest sites (n=11); grass = grassland sites (n=4).

Gelöscht: ¶
Gelöscht: 7
Gelöscht: ; Fig. 10B

The uncertainty of reconstructed RH_{MDV} values are large for all three investigated vegetation types, and again these uncertainties are probably also related to ε_{bio}, which is most likely not constant as assumed for our calculations. Moreover, microclimate variability is underestimated in our approach. As mentioned in sections 2.4.2 and 3.7, in the coupled approach not only the source water of the plants is equated with (weighted) mean annual precipitation, but also an isotopic equilibrium between the source water and the (local) atmospheric water vapour is assumed. However, in areas with distinct seasonality this might be not fully valid. To account for this lack of equilibrium between precipitation and local atmospheric water vapour, apparent ε values can be calculated with data from Jacob and Sonntag, (1991). As shown by Hepp et al. (2018) those values can be used to achieve alternative RH reconstructions based on the coupled $\delta^2H_{n\text{-alkane}}$-$\delta^{18}O_{sugar}$ approach. Such calculated RH_{MDV} values are on average 1.5% more negative than the original values. However, this difference in RH is far below the analytical uncertainties of the compound-specific biomarker isotope analysis.

Finally, the integration time of the investigated topsoils has to be discussed. Unfortunately, no ^{14}C dates are available for the soil samples. However, most likely the organic matter has been built up over a longer timescale than the available climate data, which is used for comparison. In combination with vegetation changes/management changes throughout that period, this could surely lead to a less tight relationship of the reconstructions compared to the climate station data. Root input of arabinose and xylose seems to be of minor relevance in our topsoil samples. Otherwise, the reconstructed $\delta^{18}O_{sugar}$ values would be too negative resulting in RH_{MDV} overestimations, which is not observed.

4 Conclusions

We were able to show that

(i) the vegetation type does not significantly influence the brGDGT concentrations and proxies, yet the coniferous sites tend to have higher brGDGT concentrations, BIT indices and CBT-MBT' ratios, while grass sites tend to be lowest.

(ii) CBT faithfully records soil pH with a median ΔpH of 0.6 ±0.6, The CBT overestimates the real pH particularly at the forest sites.

(iii) CBT-MBT'-derived T_{MA} reflect the climate station-derived T_{MA} values with a median ΔT_{MA} of 0.5°C ±2.4, but again slightly too high reconstruction for the forest sites were observed.

(iv) differences in the apparent fractionation between the investigated vegetation types could caused by "signal damping" or variable ε_{bio} along with vegetation types, which are indistinguishable here.

(v) the reconstructed $\delta^2H_{source\text{-}water}$ and $\delta^{18}O_{source\text{-}water}$ reflects the $\delta^2H_{GIPR,OIPC}$ and $\delta^{18}O_{GIPR,OIPC}$ with a systematic offset for δ^2H of ~-21‰ ±22 and for $\delta^{18}O$ of ~-2.9‰ ±2.8 (based on overall medians of $\Delta\delta^2H$, $\delta^{18}O$). This is caused by too negative reconstructions for coniferous and grass sites. For coniferous sites, this can be explained with *n*-alkanes originating from understory grasses. As for the grass sites, the "signal damping" or variable ε_{bio} along with vegetation types more effect δ^2H

Gelöscht: 6

Gelöscht: /

Gelöscht: -

Gelöscht: are

Gelöscht: , i.e. the grasses do not see and record the full evaporative enrichment of leaf water.

Gelöscht: /

Gelöscht: /

Gelöscht: /

Gelöscht: /

Gelöscht: ,

Gelöscht: and f

than $\delta^{18}O$. This leads to too negative reconstructed $\delta^{2}H_{leaf\text{-}water}$ values and thus to too negative $\delta^{2}H_{source\text{-}water}$ and $\delta^{18}O_{source\text{-}water}$ reconstructions.

(vi) reconstructed (biomarker-based) RH_{MDV} values tend to underestimate climate station-derived RH_{MDV} values (ΔRH_{MDV} = ~ -17% ±12). For coniferous sites the underestimations are strongest, which can be explained with understory grasses being the main source of *n*-alkanes for the investigated soils under coniferous forests.

Overall, our study highlights the great potential of GDGTs and the coupled $\delta^{2}H_{n\text{-}alkane}$-$\delta^{18}O_{sugar}$ approach for more quantitative paleoclimate reconstructions. Taking into account effects of different vegetation types improves correlations and reconstructions. This holds particularly true for the coupled $\delta^{2}H_{n\text{-}alkane}$-$\delta^{18}O_{sugar}$ approach, which is affected by "signal damping" of the grass vegetation or variable ε_{bio} along with vegetation types. Assuming constant biosynthetic fractionation is likely a considerable source of uncertainty and should be in focus in future field and/or modelling studies. Climate chamber experiments would be very useful to further evaluate and refine the coupled $\delta^{2}H_{n\text{-}alkane}$-$\delta^{18}O_{sugar}$ approach, because uncertainties related to microclimate variability can be reduced. Field experiments like ours suffer from the fact that biomarker pools in the sampled topsoils may have been affected by past vegetation and climate changes.

Gelöscht: /

Gelöscht: of the grass vegetation

Acknowledgements

We thank L. Wüthrich, H. Veit, T. Sprafke, A. Groos (all University of Bern), A. Kühnel (Technical University of Munich) for constructive discussions and statistical advices, and M. Schaarschmidt (University of Bayreuth), C. Heinrich and M. Benesch (Martin-Luther-University Halle-Wittenberg) for laboratory assistance during $\delta^{18}O_{sugar}$ analysis and pH measurements, respectively. The Swiss National Science Foundation (PP00P2 150590) funded this research. J. Hepp greatly acknowledges the support by the German Federal Environmental Foundation (DBU) in form of his PhD-fellowship.

References

Allison, G. B., Gat, J. R. and Leaney, F. W. J.: The relationship between deuterium and oxygen-18 delta values in leaf water, Chemical Geology, 58, 145–156, 1985.

Amelung, W., Cheshire, M. V. and Guggenberger, G.: Determination of neutral and acidic sugars in soil by capillary gas-liquid chromatography after trifluoroacetic acid hydrolysis, Soil Biology and Biochemistry, 28(12), 1631–1639, 1996.

Anderson, V. J., Shanahan, T. M., Saylor, J. E., Horton, B. K. and Mora, A. R.: Sources of local and regional variability in the MBT'/CBT paleotemperature proxy: Insights from a modern elevation transect across the Eastern Cordillera of Colombia, Organic Geochemistry, 69, 42–51, doi:10.1016/j.orggeochem.2014.01.022, 2014.

Awe, G. O., Reichert, J. M. and Wendroth, O. O.: Temporal variability and covariance structures of soil temperature in a sugarcane field under different management practices in southern Brazil, Soil and Tillage Research, 150, 93–106,

745 doi:10.1016/j.still.2015.01.013, 2015.

746 Bariac, T., Gonzalez-Dunia, J., Katerji, N., Béthenod, O., Bertolini, J. M. and Mariotti, A.:
747 Spatial variation of the isotopic composition of water (^{18}O, ^{2}H) in the soil-plant-
748 atmosphere system, 2. Assessment under field conditions, Chemical Geology, 115, 317–
749 333, 1994.

750 Bowen, G. J.: The Online Isotopes in Precipitation Calculator, version 3.1., 2018.

751 Bowen, G. J. and Revenaugh, J.: Interpolating the isotopic composition of modern meteoric
752 precipitation, Water Resources Research, 39(10), 1–13, doi:10.1029/2003WR002086,
753 2003.

754 Brincat, D., Yamada, K., Ishiwatari, R., Uemura, H. and Naraoka, H.: Molecular-isotopic
755 stratigraphy of long-chain *n*-alkanes in Lake Baikal Holocene and glacial age sediments,
756 Organic Geochemistry, 31(4), 287–294, doi:10.1016/S0146-6380(99)00164-3, 2000.

757 Cappelen, J.: Danish Climatological Normals 1971-2000 - for selected stations., 2002.

758 Cernusak, L. A., Wong, S. C. and Farquhar, G. D.: Oxygen isotope composition of phloem sap
759 in relation to leaf water in Ricinus communis, Functional Plant Biology, 30(10), 1059–
760 1070, 2003.

761 Cernusak, L. A., Barbour, M. M., Arndt, S. K., Cheesman, A. W., English, N. B., Feild, T. S.,
762 Helliker, B. R., Holloway-Phillips, M. M., Holtum, J. A. M., Kahmen, A., Mcinerney, F.
763 A., Munksgaard, N. C., Simonin, K. A., Song, X., Stuart-Williams, H., West, J. B. and
764 Farquhar, G. D.: Stable isotopes in leaf water of terrestrial plants, Plant Cell and
765 Environment, 39(5), 1087–1102, doi:10.1111/pce.12703, 2016.

766 Christoph, H., Eglinton, T. I., Zech, W., Sosin, P. and Zech, R.: A 250 ka leaf-wax δD record
767 from a loess section in Darai Kalon , Southern Tajikistan, Quaternary Science Reviews,
768 208, 118–128, doi:10.1016/j.quascirev.2019.01.019, 2019.

769 Coffinet, S., Huguet, A., Anquetil, C., Derenne, S., Pedentchouk, N., Bergonzini, L.,
770 Omuombo, C., Williamson, D., Jones, M., Majule, A. and Wagner, T.: Evaluation of
771 branched GDGTs and leaf wax n-alkane $\delta^{2}H$ as (paleo) environmental proxies in East
772 Africa, Geochimica et Cosmochimica Acta, 198, 182–193,
773 doi:10.1016/j.gca.2016.11.020, 2017.

774 Cormier, M.-A., Werner, R. A., Sauer, P. E., Gröcke, D. R., M.C., L., Wieloch, T., Schleucher,
775 J. and Kahmen, A.: ^{2}H fractiontions during the biosynthesis of carbohydrates and lipids
776 imprint a metabolic signal on the $\delta^{2}H$ values of plant organic compounds, New
777 Phytologist, 218(2), 479–491, doi:10.1111/nph.15016, 2018.

778 Craig, H.: Isotopic Variations in Meteoric Waters, Science, 133, 1702–1703, 1961.

779 Dang, X., Yang, H., Naafs, B. D. A., Pancost, R. D. and Xie, S.: Evidence of moisture control
780 on the methylation of branched glycerol dialkyl glycerol tetraethers in semi-arid and arid
781 soils, Geochimica et Cosmochimica Acta, 189, 24–36, doi:10.1016/j.gca.2016.06.004,
782 2016.

783 Dansgaard, W.: Stable isotopes in precipitation, Tellus, 16(4), 436–468, doi:10.1111/j.2153-
784 3490.1964.tb00181.x, 1964.

785 Dawson, T. E., Mambelli, S., Plamboeck, A. H., Templer, P. H. and Tu, K. P.: Stable Isotopes
786 in Plant Ecology, Annual Review of Ecology and Systematics, 33(1), 507–559,
787 doi:10.1146/annurev.ecolsys.33.020602.095451, 2002.

788 Diefendorf, A. F. and Freimuth, E. J.: Extracting the most from terrestrial plant-derived *n*-alkyl
789 lipids and their carbon isotopes from the sedimentary record: A review, Organic
790 Geochemistry, 103(January), 1–21, doi:10.1016/j.orggeochem.2016.10.016, 2016.

791 Dirghangi, S. S., Pagani, M., Hren, M. T. and Tipple, B. J.: Distribution of glycerol dialkyl
792 glycerol tetraethers in soils from two environmental transects in the USA, Organic
793 Geochemistry, 59, 49–60, doi:10.1016/j.orggeochem.2013.03.009, 2013.

794 Dubbert, M., Cuntz, M., Piayda, A., Maguás, C. and Werner, C.: Partitioning evapotranspiration
795 - Testing the Craig and Gordon model with field measurements of oxygen isotope ratios
796 of evaporative fluxes, Journal of Hydrology, 496, 142–153,
797 doi:10.1016/j.jhydrol.2013.05.033, 2013.

798 DWD Climate Data Center: Historical annual precipitation observations for Germany. [online]
799 Available from: ftp://ftp-
800 cdc.dwd.de/pub/CDC/observations_germany/climate/hourly/precipitation/historical/
801 (Accessed 20 September 2018a), 2018.

802 DWD Climate Data Center: Historical hourly station observations of 2m air temperature and
803 humidity for Germany. [online] Available from: ftp://ftp-
804 cdc.dwd.de/pub/CDC/observations_germany/climate/hourly/air_temperature/historical/
805 (Accessed 19 September 2018b), 2018.

806 Eglinton, T. I. and Eglinton, G.: Molecular proxies for paleoclimatology, Earth and Planetary
807 Science Letters, 275(1), 1–16, 2008.

808 Feakins, S. J. and Sessions, A. L.: Controls on the D/H ratios of plant leaf waxes in an arid
809 ecosystem, Geochimica et Cosmochimica Acta, 74(7), 2128–2141,
810 doi:http://dx.doi.org/10.1016/j.gca.2010.01.016, 2010.

811 Feakins, S. J., Bentley, L. P., Salinas, N., Shenkin, A., Blonder, B., Goldsmith, G. R., Ponton,
812 C., Arvin, L. J., Wu, M. S., Peters, T., West, A. J., Martin, R. E., Enquist, B. J., Asner, G.
813 P. and Malhi, Y.: Plant leaf wax biomarkers capture gradients in hydrogen isotopes of
814 precipitation from the Andes and Amazon, Geochimica et Cosmochimica Acta, 182, 155–
815 172, doi:10.1016/j.gca.2016.03.018, 2016.

816 Freimuth, E. J., Diefendorf, A. F. and Lowell, T. V.: Hydrogen isotopes of *n*-alkanes and *n*-
817 alkanoic acids as tracers of precipitation in a temperate forest and implications for
818 paleorecords, Geochimica et Cosmochimica Acta, 206, 166–183,
819 doi:10.1016/j.gca.2017.02.027, 2017.

820 Frich, P., Rosenørn, S., Madsen, H. and Jensen, J. J.: Observed Precipitation in Denmark, 1961-
821 90., 1997.

822 Gamarra, B., Sachse, D. and Kahmen, A.: Effects of leaf water evaporative ^{2}H-enrichment and
823 biosynthetic fractionation on leaf wax *n*-alkane δ^{2}H values in C3 and C4 grasses, Plant,
824 Cell and Environment Environment, 39, 2390–2403, doi:10.1111/pce.12789, 2016.

825 Gat, J. R.: Comments on the Stable Isotope Method in Regional Groundwater Investigations,
826 Water Resources Research, 7(4), 980–993, doi:10.1029/WR007i004p00980, 1971.

827 van Geldern, R., Baier, A., Subert, H. L., Kowol, S., Balk, L. and Barth, J. A. C.: (Table S1)
828 Stable isotope composition of precipitation sampled at Erlangen, Germany between 2010
829 and 2013 for station GeoZentrum located at Erlangen city center, in In supplement to: van
830 Geldern, R et al. (2014): Pleistocene paleo-groundwater as a pristine fresh water resource
831 in southern Germany – evidence from stable and radiogenic isotopes. Science of the Total

832 Environment, 496, 107-115, https://doi.org/10.1016/j., PANGAEA., 2014.

833 Guggenberger, G., Christensen, B. T. and Zech, W.: Land-use effects on the composition of
834 organic matter in particle-size separates of soil: I. Lignin and carbohydrate signature,
835 European Journal of Soil Science, 45(December), 449–458, 1994.

836 Helliker, B. R. and Ehleringer, J. R.: Grass blades as tree rings: environmentally induced
837 changes in the oxygen isotope ratio of cellulose along the length of grass blades, New
838 Phytologist, 155, 417–424, 2002.

839 Hepp, J., Rabus, M., Anhäuser, T., Bromm, T., Laforsch, C., Sirocko, F., Glaser, B. and Zech,
840 M.: A sugar biomarker proxy for assessing terrestrial versus aquatic sedimentary input,
841 Organic Geochemistry, 98, 98–104, doi:10.1016/j.orggeochem.2016.05.012, 2016.

842 Hepp, J., Wüthrich, L., Bromm, T., Bliedtner, M., Schäfer, I. K., Glaser, B., Rozanski, K.,
843 Sirocko, F., Zech, R. and Zech, M.: How dry was the Younger Dryas? Evidence from a
844 coupled δ^2H-δ^{18}O biomarker paleohygrometer, applied to the Lake Gemündener Maar
845 sediments, Western Eifel, Germany, Climate of the Past Discussions, (September), 1–44,
846 doi:10.5194/cp-2018-114, 2018.

847 Herrmann, A., Maloszewski, P. and Stichler, W.: Changes of ^{18}O contents of precipitation water
848 during seepage in the unsaturated zone, in Proceedings of International Symposium on
849 Groundwater Monitoring and Management, 23 - 28 March, p. 22, Institut of Water
850 Management Berlin (GDR) with support of UNESCO, Dresden., 1987.

851 Hopmans, E. C., Weijers, J. W. H., Schefuß, E., Herfort, L., Sinninghe Damsté, J. S. and
852 Schouten, S.: A novel proxy for terrestrial organic matter in sediments based on branched
853 and isoprenoid tetraether lipids, Earth and Planetary Science Letters, 224(1–2), 107–116,
854 doi:10.1016/j.epsl.2004.05.012, 2004.

855 Horita, J. and Wesolowski, D. J.: Liquid-vapor fractionation of oxygen and hydrogen isotopes
856 of water from the freezing to the critical temperature, Geochimica et Cosmochimica Acta,
857 58(16), 3425–3437, doi:http://dx.doi.org/10.1016/0016-7037(94)90096-5, 1994.

858 Hothorn, T., Bühlmann, P., Dudoit, S., Molinaro, A. and Van Der Laan, M. J.: Survival
859 ensembles, Biostatistics, 7(3), 355–373, doi:10.1093/biostatistics/kxj011, 2006.

860 Hou, J., D'Andrea, W. J. and Huang, Y.: Can sedimentary leaf waxes record D/H ratios of
861 continental precipitation? Field, model, and experimental assessments, Geochimica et
862 Cosmochimica Acta, 72, 3503–3517, doi:10.1016/j.gca.2008.04.030, 2008.

863 Huguet, A., Fosse, C., Metzger, P., Fritsch, E. and Derenne, S.: Occurrence and distribution of
864 extractable glycerol dialkyl glycerol tetraethers in podzols, Organic Geochemistry, 41(3),
865 291–301, doi:10.1016/j.orggeochem.2009.10.007, 2010a.

866 Huguet, A., Fosse, C., Laggoun-Défarge, F., Toussaint, M. L. and Derenne, S.: Occurrence and
867 distribution of glycerol dialkyl glycerol tetraethers in a French peat bog, Organic
868 Geochemistry, 41(6), 559–572, doi:10.1016/j.orggeochem.2010.02.015, 2010b.

869 IAEA/WMO: Global Network of Isotopes in Precipitation. The GNIP Database., 2015.

870 IAEA/WMO: Global Network of Isotopes in Precipitation. The GNIP Database., 2018.

871 Jacob, H. and Sonntag, C.: An 8-year record of the seasonal- variation of ^{2}H and ^{18}O in
872 atmospheric water vapor and precipitation at Heidelberg, Tellus, 43B(3), 291–300, 1991.

873 De Jonge, C., Hopmans, E. C., Zell, C. I., Kim, J. H., Schouten, S. and Sinninghe Damsté, J.

S.: Occurrence and abundance of 6-methyl branched glycerol dialkyl glycerol tetraethers in soils: Implications for palaeoclimate reconstruction, Geochimica et Cosmochimica Acta, 141, 97–112, doi:10.1016/j.gca.2016.03.038, 2014.

Kahmen, A., Schefuß, E. and Sachse, D.: Leaf water deuterium enrichment shapes leaf wax *n*-alkane δD values of angiosperm plants I: Experimental evidence and mechanistic insights, Geochimica et Cosmochimica Acta, 111, 39–49, doi:10.1016/j.gca.2012.09.004, 2013.

Knapp, D. R.: Handbook of Analytical Derivatization Reactions, John Wiley & Sons, New York, Chichester, Brisbane, Toronto, Singapore., 1979.

Konecky, B., Dee, S. G. and Noone, D. C.: WaxPSM: A Forward Model of Leaf Wax Hydrogen Isotope Ratios to Bridge Proxy and Model Estimates of Past Climate, Journal of Geophysical Research: Biogeosciences, 124, 2107–2125, doi:10.1029/2018JG004708, 2019.

Laursen, E. V., Thomsen, R. S. and Cappelen, J.: Observed Air Temperature, Humidity, Pressure, Cloud Cover and Weather in Denmark - with Climatological Standard Normals, 1961-90., 1999.

Levene, H.: Robust Tests for Equality of Variances, in Contributions to Probability and Statistics: Essays in Honor of Harold Hotelling, vol. 69, edited by I. Olkin, pp. 78–92, Standford University Press, Palo Alto, California., 1960.

Liu, W. and Yang, H.: Multiple controls for the variability of hydrogen isotopic compositions in higher plant *n*-alkanes from modern ecosystems, Global Change Biology, 14(9), 2166–2177, doi:10.1111/j.1365-2486.2008.01608.x, 2008.

Liu, Y., Wang, J., Liu, D., Li, Z., Zhang, G., Tao, Y., Xie, J., Pan, J. and Chen, F.: Straw mulching reduces the harmful effects of extreme hydrological and temperature conditions in citrus orchards, PLoS ONE, 9(1), 1–9, doi:10.1371/journal.pone.0087094, 2014.

McInerney, F. A., Helliker, B. R. and Freeman, K. H.: Hydrogen isotope ratios of leaf wax *n*-alkanes in grasses are insensitive to transpiration, Geochimica et Cosmochimica Acta, 75(2), 541–554, doi:10.1016/j.gca.2010.10.022, 2011.

Merlivat, L.: Molecular diffusivities of $H_2{}^{16}O$, $HD^{16}O$, and $H_2{}^{18}O$ in gases, The Journal of Chemical Physics, 69(6), 2864–2871, doi:http://dx.doi.org/10.1063/1.436884, 1978.

Mueller-Niggemann, C., Utami, S. R., Marxen, A., Mangelsdorf, K., Bauersachs, T. and Schwark, L.: Distribution of tetraether lipids in agricultural soils - Differentiation between paddy and upland management, Biogeosciences, 13(5), 1647–1666, doi:10.5194/bg-13-1647-2016, 2016.

Oppermann, B. I., Michaelis, W., Blumenberg, M., Frerichs, J., Schulz, H. M., Schippers, A., Beaubien, S. E. and Krüger, M.: Soil microbial community changes as a result of long-term exposure to a natural CO_2vent, Geochimica et Cosmochimica Acta, 74(9), 2697–2716, doi:10.1016/j.gca.2010.02.006, 2010.

Pedentchouk, N. and Zhou, Y.: Factors Controlling Carbon and Hydrogen Isotope Fractionation During Biosynthesis of Lipids by Phototrophic Organisms, in Hydrocarbons, Oils and Lipids: Diversity, Origin, Chemistry and Fate. Handbook of Hydrocarbon and Lipid Microbiology, edited by H. Wilkes, pp. 1–24, Springer, Cham., 2018.

Peterse, F., van der Meer, J., Schouten, S., Weijers, J. W. H., Fierer, N., Jackson, R. B., Kim,

J. H. and Sinninghe Damsté, J. S.: Revised calibration of the MBT-CBT paleotemperature proxy based on branched tetraether membrane lipids in surface soils, Geochimica et Cosmochimica Acta, 96, 215–229, doi:10.1016/j.gca.2012.08.011, 2012.

Prietzel, J., Dechamps, N. and Spielvogel, S.: Analysis of non-cellulosic polysaccharides helps to reveal the history of thick organic surface layers on calcareous Alpine soils, Plant and Soil, 365(1–2), 93–114, doi:10.1007/s11104-012-1340-2, 2013.

R Core Team: R: A Language and Environment for Statistical Computing, [online] Available from: https://www.r-project.org/, 2015.

Rach, O., Brauer, A., Wilkes, H. and Sachse, D.: Delayed hydrological response to Greenland cooling at the onset of the Younger Dryas in western Europe, Nature Geoscience, 7(1), 109–112, doi:10.1038/ngeo2053, 2014.

Rao, Z., Zhu, Z., Jia, G., Henderson, A. C. G., Xue, Q. and Wang, S.: Compound specific δD values of long chain *n*-alkanes derived from terrestrial higher plants are indicative of the δD of meteoric waters: Evidence from surface soils in eastern China, Organic Geochemistry, 40(8), 922–930, doi:http://dx.doi.org/10.1016/j.orggeochem.2009.04.011, 2009.

Romero-Viana, L., Kienel, U. and Sachse, D.: Lipid biomarker signatures in a hypersaline lake on Isabel Island (Eastern Pacific) as a proxy for past rainfall anomaly (1942-2006AD), Palaeogeography, Palaeoclimatology, Palaeoecology, 350–352, 49–61, doi:10.1016/j.palaeo.2012.06.011, 2012.

Sachse, D., Radke, J. and Gleixner, G.: Hydrogen isotope ratios of recent lacustrine sedimentary *n*-alkanes record modern climate variability, Geochimica et Cosmochimica Acta, 68(23), 4877–4889, doi:http://dx.doi.org/10.1016/j.gca.2004.06.004, 2004.

Sachse, D., Radke, J. and Gleixner, G.: δD values of individual *n*-alkanes from terrestrial plants along a climatic gradient – Implications for the sedimentary biomarker record, Organic Geochemistry, 37, 469–483, doi:10.1016/j.orggeochem.2005.12.003, 2006.

Sachse, D., Billault, I., Bowen, G. J., Chikaraishi, Y., Dawson, T. E., Feakins, S. J., Freeman, K. H., Magill, C. R., McInerney, F. A., van der Meer, M. T. J., Polissar, P., Robins, R. J., Sachs, J. P., Schmidt, H.-L., Sessions, A. L., White, J. W. C. and West, J. B.: Molecular Paleohydrology: Interpreting the Hydrogen-Isotopic Composition of Lipid Biomarkers from Photosynthesizing Organisms, Annual Reviews, 40, 221–249, doi:10.1146/annurev-earth-042711-105535, 2012.

Schäfer, I. K., Lanny, V., Franke, J., Eglinton, T. I., Zech, M., Vysloužilová, B. and Zech, R.: Leaf waxes in litter and topsoils along a European transect, SOIL, 2, 551–564, doi:10.5194/soil-2-551-2016, 2016.

Schlotter, D.: The spatio-temporal distribution of $\delta^{18}O$ and $\delta^{2}H$ of precipitation in Germany - an evaluation of regionalization methods, Albert-Ludwigs-Universität Freiburg im Breisgau. [online] Available from: http://www.hydrology.uni-freiburg.de/abschluss/Schlotter_D_2007_DA.pdf, 2007.

Schmidt, H.-L., Werner, R. A. and Roßmann, A.: ^{18}O Pattern and biosynthesis of natural plant products, Phytochemistry, 58(1), 9–32, doi:http://dx.doi.org/10.1016/S0031-9422(01)00017-6, 2001.

Schmidt, H.-L., Werner, R. A. and Eisenreich, W.: Systematics of ^{2}H patterns in natural compounds and its importance for the elucidation of biosynthetic pathways,

Phytochemistry Reviews, 2(1–2), 61–85, doi:10.1023/B:PHYT.0000004185.92648.ae, 2003.

Schouten, S., Hopmans, E. C. and Sinninghe Damsté, J. S.: The organic geochemistry of glycerol dialkyl glycerol tetraether lipids: A review, Organic Geochemistry, 54, 19–61, doi:10.1016/j.orggeochem.2012.09.006, 2013.

Schreuder, L. T., Beets, C. J., Prins, M. A., Hatté, C. and Peterse, F.: Late Pleistocene climate evolution in Southeastern Europe recorded by soil bacterial membrane lipids in Serbian loess, Palaeogeography, Palaeoclimatology, Palaeoecology, 449, 141–148, doi:10.1016/j.palaeo.2016.02.013, 2016.

Sessions, A. L., Burgoyne, T. W., Schimmelmann, A. and Hayes, J. M.: Fractionation of hydrogen isotopes in lipid biosynthesis, Organic Geochemistry, 30, 1193–1200, 1999.

Shapiro, S. S. and Wilk, M. B.: An Analysis of Variance Test for Normality, Biometrika, 52(3/4), 591–611, doi:/biomet/52.3-4.591, 1965.

Sternberg, L. S. L.: Comment on "Oxygen isotope ratios ($^{18}O/^{16}O$) of hemicellulose-derived sugar biomarkers in plants, soils and sediments as paleoclimate proxy I: Insight from a climate chamber experiment" by Zech et al. (2014), Geochimica et Cosmochimica Acta, 141, 677–679, doi:10.1016/j.gca.2014.04.051, 2014.

Strobl, C., Boulesteix, A. L., Zeileis, A. and Hothorn, T.: Bias in random forest variable importance measures: Illustrations, sources and a solution, BMC Bioinformatics, 8, doi:10.1186/1471-2105-8-25, 2007.

Strobl, C., Boulesteix, A. L., Kneib, T., Augustin, T. and Zeileis, A.: Conditional variable importance for random forests, BMC Bioinformatics, 9, 1–11, doi:10.1186/1471-2105-9-307, 2008.

Stumpp, C., Klaus, J. and Stichler, W.: Analysis of long-term stable isotopic composition in German precipitation, Journal of Hydrology, 517, 351–361, doi:10.1016/j.jhydrol.2014.05.034, 2014.

Sun, C. J., Zhang, C. L., Li, F. Y., Wang, H. Y. and Liu, W. G.: Distribution of branched glycerol dialkyl glycerol tetraethers in soils on the Northeastern Qinghai-Tibetan Plateau and possible production by nitrite-reducing bacteria, Science China Earth Sciences, 59(9), 1834–1846, doi:10.1007/s11430-015-0230-2, 2016.

Swedish Meteorological and Hydrological Institute: SMHI Open Data Meteorological Observations., 2018.

Tipple, B. J., Berke, M. A., Hambach, B., Roden, J. S. and Ehleringer, J. R.: Predicting leaf wax *n*-alkane $^{2}H/^{1}H$ ratios: Controlled water source and humidity experiments with hydroponically grown trees confirm predictions of Craig-Gordon model, Plant, Cell and Environment, 38(6), 1035–1047, doi:10.1111/pce.12457, 2015.

Tuthorn, M., Zech, M., Ruppenthal, M., Oelmann, Y., Kahmen, A., del Valle, H. F., Wilcke, W. and Glaser, B.: Oxygen isotope ratios ($^{18}O/^{16}O$) of hemicellulose-derived sugar biomarkers in plants, soils and sediments as paleoclimate proxy II: Insight from a climate transect study, Geochimica et Cosmochimica Acta, 126, 624–634, doi:http://dx.doi.org/10.1016/j.gca.2013.11.002, 2014.

Tuthorn, M., Zech, R., Ruppenthal, M., Oelmann, Y., Kahmen, A., del Valle, H. F., Eglinton, T., Rozanski, K. and Zech, M.: Coupling $\delta^{2}H$ and $\delta^{18}O$ biomarker results yields

information on relative humidity and isotopic composition of precipitation - a climate transect validation study, Biogeosciences, 12, 3913–3924, doi:10.5194/bg-12-3913-2015, 2015.

Umweltbundesamt GmbH: Erhebung der Wassergüte in Österreich gemäß Hydrographiegesetz i.d.F. des BGBl. Nr. 252/90 (gültig bis Dezember 2006) bzw. Gewässerzustandsüberwachung in Österreich gemäß Wasserrechtsgesetz, BGBl. I Nr. 123/06, i.d.g.F.; BMLFUW, Sektion IV / Abteilung 3 N. [online] Available from: https://wasser.umweltbundesamt.at/h2odb/fivestep/abfrageQdPublic.xhtml (Accessed 20 September 2018), 2018.

Walker, C. D. and Brunel, J.-P.: Examining Evapotranspiration in a Semi-Arid Region using Stable Isotopes of Hydrogen and Oxygen, Journal of Hydrology, 118, 55–75, 1990.

Wang, C., Hren, M. T., Hoke, G. D., Liu-Zeng, J. and Garzione, C. N.: Soil *n*-alkane δD and glycerol dialkyl glycerol tetraether (GDGT) distributions along an altitudinal transect from southwest China: Evaluating organic molecular proxies for paleoclimate and paleoelevation, Organic Geochemistry, 107, 21–32, doi:10.1016/j.orggeochem.2017.01.006, 2017.

Wang, H., Liu, W., Zhang, C. L., Liu, Z. and He, Y.: Branched and isoprenoid tetraether (BIT) index traces water content along two marsh-soil transects surrounding Lake Qinghai: Implications for paleo-humidity variation, Organic Geochemistry, 59, 75–81, doi:10.1016/j.orggeochem.2013.03.011, 2013.

Weijers, J. W. H., Schouten, S., Spaargaren, O. C. and Sinninghe Damsté, J. S.: Occurrence and distribution of tetraether membrane lipids in soils: Implications for the use of the TEX_{86} proxy and the BIT index, Organic Geochemistry, 37(12), 1680–1693, doi:10.1016/j.orggeochem.2006.07.018, 2006.

Weijers, J. W. H., Schouten, S., van den Donker, J. C., Hopmans, E. C. and Sinninghe Damsté, J. S.: Environmental controls on bacterial tetraether membrane lipid distribution in soils, Geochimica et Cosmochimica Acta, 71(3), 703–713, doi:10.1016/j.gca.2006.10.003, 2007.

Weijers, J. W. H., Wiesenberg, G. L. B., Bol, R., Hopmans, E. C. and Pancost, R. D.: Carbon isotopic composition of branched tetraether membrane lipids in soils suggest a rapid turnover and a heterotrophic life style of their source organism(s), Biogeosciences, 7(9), 2959–2973, doi:10.5194/bg-7-2959-2010, 2010.

Weijers, J. W. H., Steinmann, P., Hopmans, E. C., Schouten, S. and Sinninghe Damsté, J. S.: Bacterial tetraether membrane lipids in peat and coal: Testing the MBT-CBT temperature proxy for climate reconstruction, Organic Geochemistry, 42(5), 477–486, doi:10.1016/j.orggeochem.2011.03.013, 2011.

Xie, S., Pancost, R. D., Chen, L., Evershed, R. P., Yang, H., Zhang, K., Huang, J. and Xu, Y.: Microbial lipid records of highly alkaline deposits and enhanced aridity associated with significant uplift of the Tibetan Plateau in the Late Miocene, Geology, 40(4), 291–294, doi:10.1130/G32570.1, 2012.

Zech, M. and Glaser, B.: Compound-specific $\delta^{18}O$ analyses of neutral sugars in soils using gas chromatography-pyrolysis-isotope ratio mass spectrometry: problems, possible solutions and a first application, Rapid Communications in Mass Spectrometry, 23, 3522–3532, doi:10.1002/rcm, 2009.

Formatiert: Deutsch (Deutschland)

Zech, M., Rass, S., Buggle, B., Löscher, M. and Zöller, L.: Reconstruction of the late Quaternary paleoenvironments of the Nussloch loess paleosol sequence, Germany, using n-alkane biomarkers, Quaternary Research, 78(2), 226–235, doi:10.1016/j.yqres.2012.05.006, 2012a.

Zech, M., Kreutzer, S., Goslar, T., Meszner, S., Krause, T., Faust, D. and Fuchs, M.: Technical Note: *n*-Alkane lipid biomarkers in loess: post-sedimentary or syn-sedimentary?, Discussions, Biogeosciences, 9, 9875–9896, doi:10.5194/bgd-9-9875-2012, 2012b.

Zech, M., Tuthorn, M., Detsch, F., Rozanski, K., Zech, R., Zöller, L., Zech, W. and Glaser, B.: A 220 ka terrestrial $\delta^{18}O$ and deuterium excess biomarker record from an eolian permafrost paleosol sequence, NE-Siberia, Chemical Geology, doi:10.1016/j.chemgeo.2013.10.023, 2013.

Zech, M., Mayr, C., Tuthorn, M., Leiber-Sauheitl, K. and Glaser, B.: Reply to the comment of Sternberg on "Zech et al. (2014) Oxygen isotope ratios ($^{18}O/^{16}O$) of hemicellulose-derived sugar biomarkers in plants, soils and sediments as paleoclimate proxy I: Insight from a climate chamber experiment. GCA, Geochimica et Cosmochimica Acta, 141(0), 680–682, doi:10.1016/j.gca.2014.04.051, 2014.

Zech, M., Zech, R., Rozanski, K., Gleixner, G. and Zech, W.: Do *n*-alkane biomarkers in soils/sediments reflect the $\delta^{2}H$ isotopic composition of precipitation? A case study from Mt . Kilimanjaro and implications for paleoaltimetry and paleoclimate research, Isotopes in Environmental and Health Studies, 51(4), 508–524, doi:10.1080/10256016.2015.1058790, 2015.

Zech, R., Gao, L., Tarozo, R. and Huang, Y.: Branched glycerol dialkyl glycerol tetraethers in Pleistocene loess-paleosol sequences: Three case studies, Organic Geochemistry, 53, 38–44, doi:10.1016/j.orggeochem.2012.09.005, 2012c.

Supplementary method description

We used a random forest approach in order to predict the long term weighted means of precipitation δ^2H and the long term weighted means of precipitation $\delta^{18}O$ for each site. To implement the model, we used the cforest function of the party package (Hothorn et al., 2006; Strobl et al., 2007, 2008) of the software R (R Core Team, 2015). Predictor variables were latitude, squared latitude, longitude and altitude. The explained variance of the random forest for long term weighted means of precipitation $\delta^{18}O$ was 77.5 % and the explained variance of the random forest for long term weighted means of precipitation δ^2H was 82.3%.

Hothorn, T., Bühlmann, P., Dudoit, S., Molinaro, A. and Van Der Laan, M. J.: Survival ensembles, Biostatistics, 7(3), 355–373, doi:10.1093/biostatistics/kxj011, 2006.

R Core Team: R: A Language and Environment for Statistical Computing, [online] Available from: https://www.r-project.org/, 2015.

Strobl, C., Boulesteix, A. L., Zeileis, A. and Hothorn, T.: Bias in random forest variable importance measures: Illustrations, sources and a solution, BMC Bioinformatics, 8, doi:10.1186/1471-2105-8-25, 2007.

Strobl, C., Boulesteix, A. L., Kneib, T., Augustin, T. and Zeileis, A.: Conditional variable importance for random forests, BMC Bioinformatics, 9, 1–11, doi:10.1186/1471-2105-9-307, 2008.

Supplementary figures

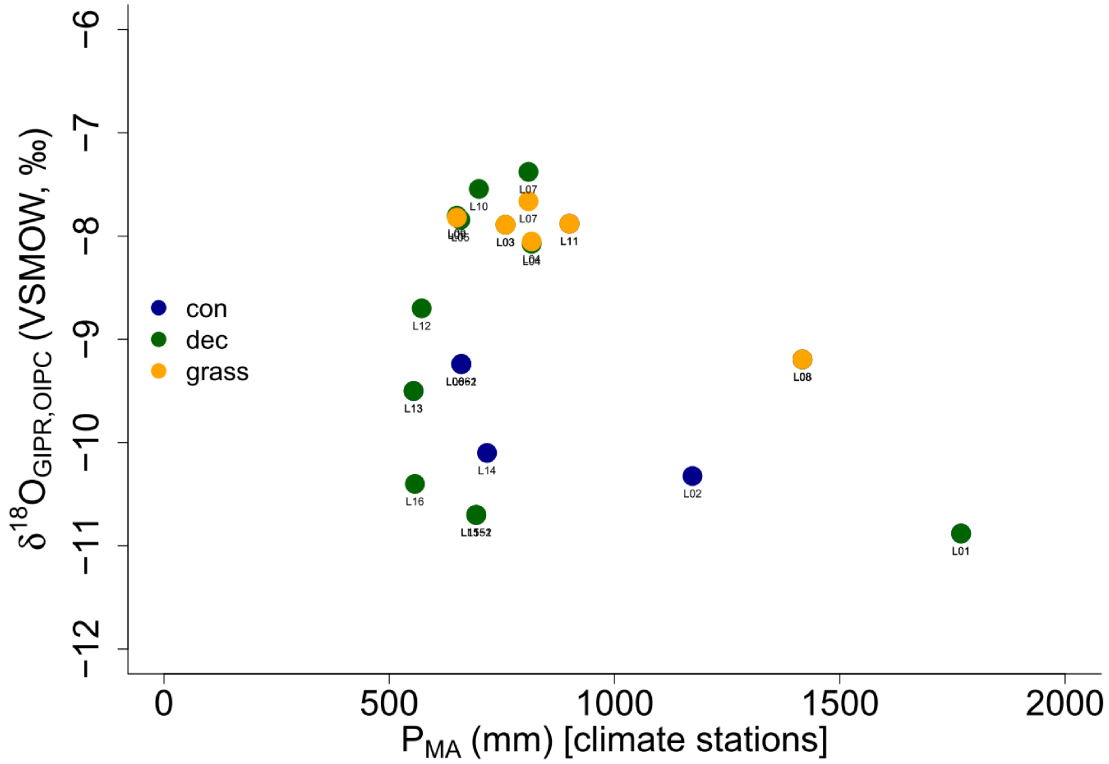

Fig. S1. Comparison between $\delta^{18}O_{GIPR,OIPC}$ values vs. P_{MA} for the three different vegetation types along the transect. All data points are marked with the location names. Abbreviations: con = coniferous forest sites (n=9); dec = deciduous forest sites (n=11); grass = grassland sites (n=4).

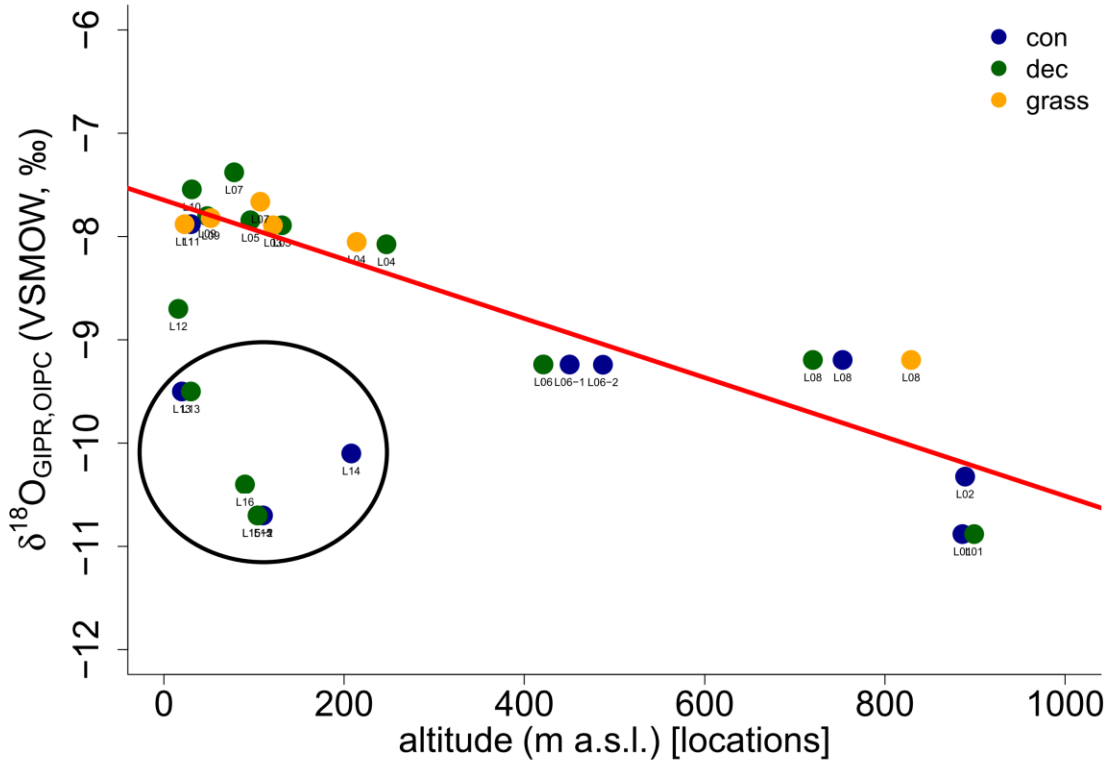

Fig. S2. Comparison between $\delta^{18}O_{GIPR,OIPC}$ values vs. location altitudes for the three different vegetation types along the transect. The red line represents the regression line throughout all German sites. All data points are marked with the location names. Swedish and Danish sites are boarded with a black circle. Abbreviations: con = coniferous forest sites (n=9); dec = deciduous forest sites (n=11); grass = grassland sites (n=4).

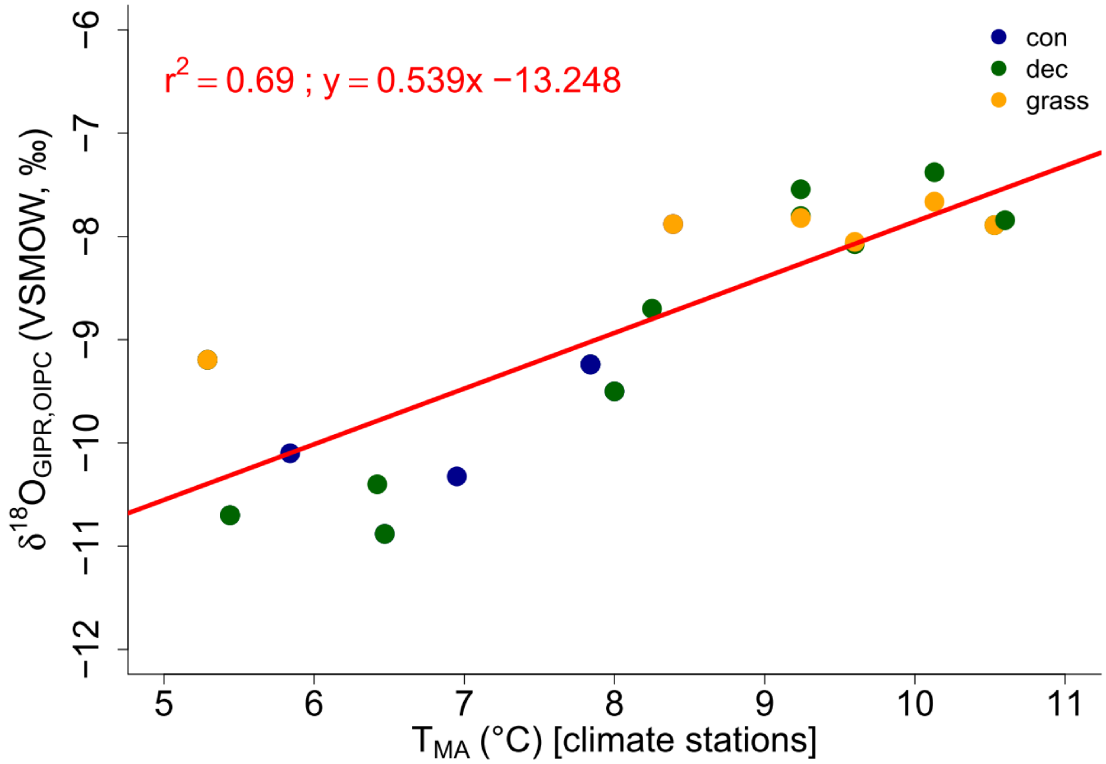

Fig. S3. Comparison between $\delta^{18}O_{GIPR,OIPC}$ values vs. T_{MA} for the three different vegetation types along the transect. The red line represents the regression line throughout all sites. Abbreviations: con = coniferous forest sites (n=9); dec = deciduous forest sites (n=11); grass = grassland sites (n=4).

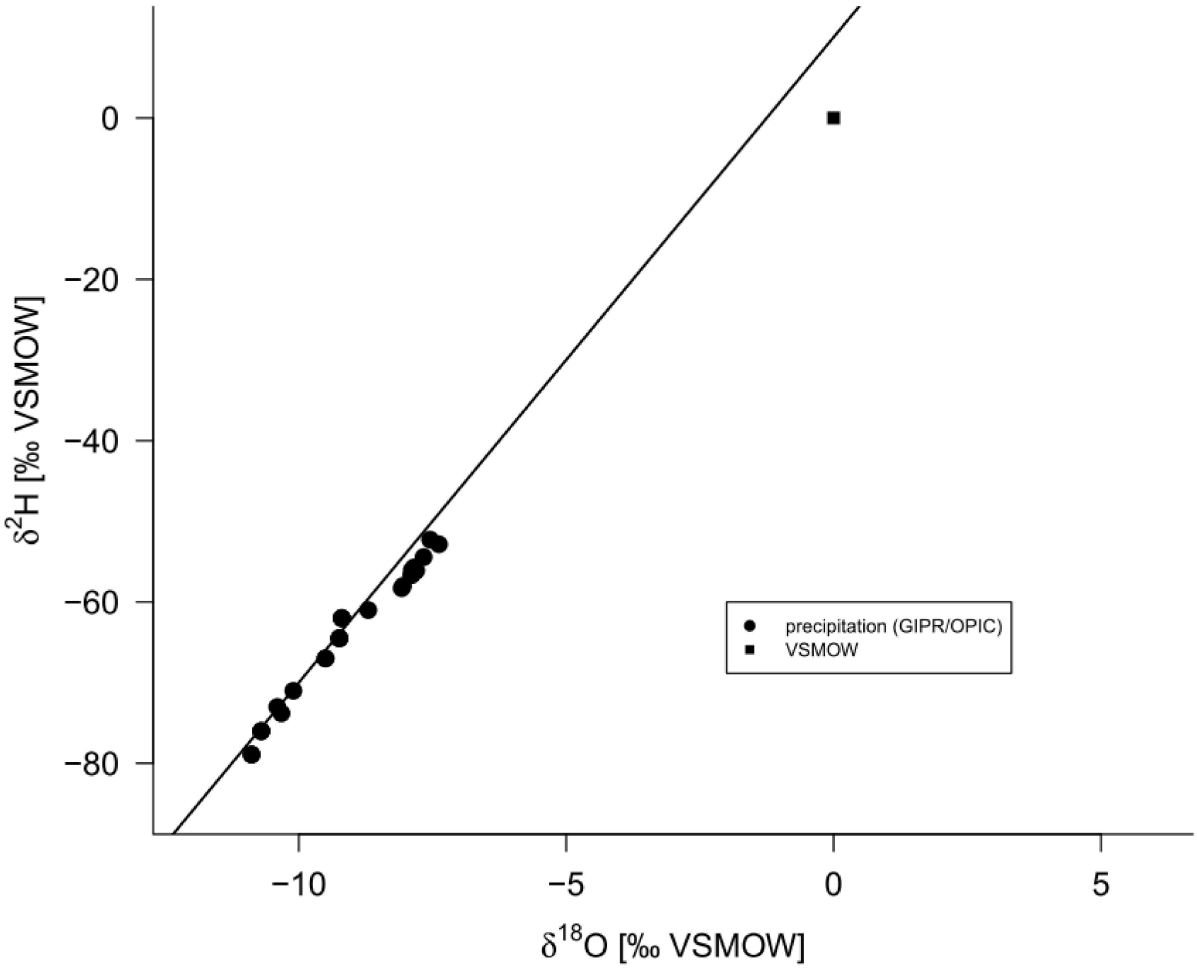

Fig. S4. $\delta^2H_{GIPR,OIPC}$ vs. $\delta^{18}O_{GIPR,OIPC}$ diagram along the transect. The black line represents the global meteoric water line (GMWL; $\delta^2H = 8 \times \delta^{18}O + 10$; Dansgaard, 1964).

Based on the values quoted in the Tabs. S1 and S2, $\delta^{18}O$ is plotted as functions of the reported environmental parameters (climate station P_{MA}, location altitude and T_{MA}; Figs. S1 to S3). It is worth to note that the five points representing Danish and Swedish sites (L12 to L16) form a separate group in Figs. S2 and S3, with clear more negative $\delta^{18}O$ values. All other (continental) sites show a regular altitude effect (decreasing $\delta^{18}O$ values with increasing altitude; red trend in Fig. S3). All Danish and Swedish isotope signatures of precipitation are shifted from the trend line by ca 2 to 2.5‰ towards more negative $\delta^{18}O$ values. One would rather expect more enriched values due to relative proximity to the sea. It should be noted that those values were derived from OIPC, while the $\delta^{18}O$ data for the German sites is derived from GNIP/ANIP data (see section 2.2 for more details). The precipitation $\delta^{18}O$ shows the expected relationship with T_{MA} (Fig. S4). The slope of this relationship (ca. 0.54‰/°C) is in the range of the slope of δ-T spatial relationship observed at mid latitudes of the northern hemisphere (e.g. Rozanski et al., 1993). It is apparent from the above Fig. S5 that the data points plot along the GMWL. Only more positive $\delta^{18}O$ values cluster below the line, indicating most probably some evaporation enrichment effects (partial evaporation of raindrops and/or evaporation effects in the rain gauges).

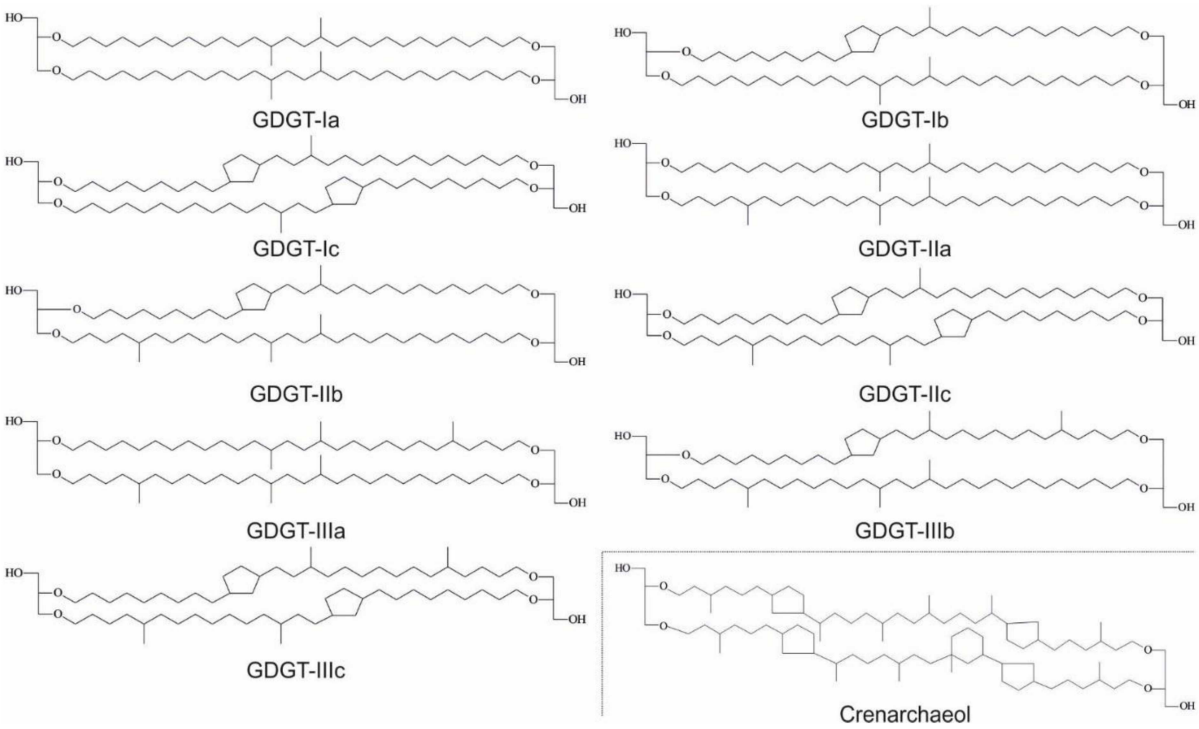

Fig. S5. Structures of brGDGTs and Crenarchaeol mentioned.

Literature

Dansgaard, W.: Stable isotopes in precipitation, Tellus, 16(4), 436–468, doi:10.1111/j.2153-3490.1964.tb00181.x, 1964.

Rozanski, K., Araguás-Araguás, L. and Gonfiantini, R.: Isotopic patterns in modern global precipitation, Climate change in continental isotopic records, 1–36, 1993.

Supplementary data

Tab. S1. Location characterization, GIPR and OIPC data.

Location	Vegetation	Characterization	Latitude (decimal °)	Longitude (decimal °)	Altitude (m)	Precipitation δ^2H (‰)	Precipitation $\delta^{18}O$ (‰)	source
L01	con	spruce forest, steep hillside	47.4	10.3	886	-78.9	-10.9	GIPR [A,B,C,D]
L01	dec	beech forest, close to fir stand	47.4	10.3	899	-78.9	-10.9	GIPR [A,B,C,D]
L02	con	fir forest	47.8	11.0	889	-73.8	-10.3	GIPR [A,B,C,D]
L03	dec	beeches, oaks, limes, sparse pines	49.1	8.2	131	-56.6	-7.9	GIPR [A,B,C,D]
L03	grass	glade, next to farmland and fruit trees (apple, plum)	49.1	8.2	121	-56.6	-7.9	GIPR [A,B,C,D]
L04	dec	beech forest, sparse firs and oaks	49.2	9.5	247	-58.3	-8.1	GIPR [A,B,C,D]
L04	grass	grassland in the valley, next to beech forest	49.2	9.5	214	-58.0	-8.1	GIPR [A,B,C,D]
L05	dec	oak forest, sparse beeches, elms and pines	49.6	8.6	96	-55.7	-7.8	GIPR [A,B,C,D]
L06	dec	beech forest, steep hillside	50.6	10.4	421	-64.5	-9.2	GIPR [A,B,C,D]
L06-1	con1	sparse pine forest with grass layer	50.6	10.4	450	-64.5	-9.2	GIPR [A,B,C,D]
L06-2	con2	sparse larch forest with grass layer	50.6	10.4	487	-64.5	-9.2	GIPR [A,B,C,D]
L07	dec	beeches, acers, elms, oaks	50.8	7.2	78	-52.8	-7.4	GIPR [A,B,C,D]
L07	grass	heath	50.8	7.2	107	-54.4	-7.7	GIPR [A,B,C,D]
L08	con	luxuriant spruce forest	51.2	8.5	753	-62.0	-9.2	GIPR [A,B,C,D]
L08	dec	young beech forest at hillside, close to spruce stand	51.2	8.5	720	-62.0	-9.2	GIPR [A,B,C,D]
L08	grass	heath, small shrubs, close to spruce stand, initially cleared	51.2	8.5	829	-62.0	-9.2	GIPR [A,B,C,D]
L09	dec	birch forest with small oaks, sparse poplars, surrounded by farmland	52.5	9.7	48	-56.1	-7.8	GIPR [A,B,C,D]
L09	grass	next to farm track	52.5	9.7	52	-56.2	-7.8	GIPR [A,B,C,D]
L10	dec	beech-oak-forest	53.0	8.7	31	-52.3	-7.5	GIPR [A,B,C,D]
L11	con	spruce forest with larches	54.4	9.6	30	-56.0	-7.9	GIPR [A,B,C,D]
L11	grass	cow pasture, sparse oaks	54.4	9.6	23	-56.0	-7.9	GIPR [A,B,C,D]
L12	dec	acer forest with poplars, ashes and elder	55.4	10.5	16	-61.0	-8.7	OIPC [E,F,G]
L13	con	fir forest with swampy underground	56.0	12.1	20	-67.0	-9.5	OIPC [E,F,G]
L13	dec	beech forest with sparse acers, birches, loamy underground	56.0	12.1	30	-67.0	-9.5	OIPC [E,F,G]
L14	con	spruce-pine-forest with moss layer	57.6	14.2	208	-71.0	-10.1	OIPC [E,F,G]
L15	con	spruce forest, sparse birches, used as cattle run	58.9	14.9	110	-76.0	-10.7	OIPC [E,F,G]
L15-1	dec1	acers, oaks, beeches, sparse firs, on partly pebbly, partly humus-rich floor	58.9	14.9	104	-76.0	-10.7	OIPC [E,F,G]
L15-2	dec2	birch- and oak-belt at spruce forest edge, grass layer, also used as cattle run	58.9	14.9	104	-76.0	-10.7	OIPC [E,F,G]
L16	dec	oak forest, sparse birches and larches	58.5	15.0	90	-73.0	-10.4	OIPC [E,F,G]

[A] Stumpp, C., Klaus, J., Stichler, W., 2014. Analysis of long-term stable isotopic composition in German precipitation. Journal of Hydrology 517, 351–361.

[B] IAEA/WMO, 2018. Global Network of Isotopes in Precipitation. The GNIP Database, https://nucleus.iaea.org/wiser.

[C] van Geldern, R., Baier, A., Subert, H.L., Kowol, S., Balk, L., Barth, J.A.C., 2014. (Table S1) Stable isotope composition of precipitation sampled at Erlangen, Germany between 2010 and 2013 for station GeoZentrum located at Erlangen city center, in: In Supplement to: Van Geldern, R et Al. (2014): Pleistocene Paleo-Groundwater as a Pristine Fresh Water Resource in Southern Germany – Evidence from Stable and Radiogenic Isotope Science of the Total Environment, 496, 107-115, Https://Doi.Org/10.1016/J. PANGAEA.

[D] Umweltbundesamt GmbH, 2018. Erhebung der Wassergüte in Österreich gemäß Hydrographiegesetz i.d.F. des BGBl. Nr. 252/90 (gültig bis Dezember 2006) bzw. Gewässerzustandsüberwachung in Österreich gemäß Wasserrechtsgesetz, BGBl. I Nr. 123/06, i.d.g.F.; BMLFUW, Sektion IV / Abteilung 3 N, Öffentliche Qualitätsdaten-Abfrage.

[E] Bowen, G.J., 2018. The Online Isotopes in Precipitation Calculator, version 3.1, http://www.waterisotopes.org.

[F] IAEA/WMO, 2015. Global Network of Isotopes in Precipitation. The GNIP Database, https://nucleus.iaea.org/wiser.

[G] Bowen, G.J., Revenaugh, J., 2003. Interpolating the isotopic composition of modern meteoric precipitation. Water Resources Research 39, 1–13.

Tab. S2. Climate station data.

Location	Vegetation	Station ID	Name	Latitude (decimal °)	Longitude (decimal °)	Altitude (m)	Oberservation begin (YYYYMMDD)	Oberservation end (YYYYMMDD)	T_{MA} (°C)	T_{MV} (°C)	Oberservation begin (YYYYMMDD)	Oberservation end (YYYYMMDD)	T_{MDV} (°C)	Station ID	Name	Latitude (decimal °)
L01	con	3730	Oberstdorf	47.40	10.28	806	19480101	20171231	6.5 [A]	11.5 [A]	n.n.	n.n.	14.2 [A]	n.n.	n.n.	n.n.
L01	dec	3730	Oberstdorf	47.40	10.28	806	19480101	20171231	6.5 [A]	11.5 [A]	n.n.	n.n.	14.2 [A]	n.n.	n.n.	n.n.
L02	con	2290	Hohenpeißenberg	47.80	11.01	977	19470101	20171231	7.0 [A]	11.4 [A]	n.n.	n.n.	12.7 [A]	n.n.	n.n.	n.n.
L03	dec	2522	Karlsruhe	49.04	8.36	112	19480101	20081102	10.5 [A]	15.3 [A]	n.n.	n.n.	17.8 [A]	n.n.	n.n.	n.n.
L03	grass	2522	Karlsruhe	49.04	8.36	112	19480101	20081102	10.5 [A]	15.3 [A]	n.n.	n.n.	17.8 [A]	n.n.	n.n.	n.n.
L04	dec	3761	Öhringen	49.21	9.52	276	19550101	20171231	9.6 [A]	14.4 [A]	n.n.	n.n.	16.8 [A]	n.n.	n.n.	n.n.
L04	grass	3761	Öhringen	49.21	9.52	276	19550101	20171231	9.6 [A]	14.4 [A]	n.n.	n.n.	16.8 [A]	n.n.	n.n.	n.n.
L05	dec	5906	Mannheim	49.51	8.56	98	19480101	20171231	10.6 [A]	15.4 [A]	n.n.	n.n.	17.9 [A]	n.n.	n.n.	n.n.
L06	dec	3231	Meiningen	50.56	10.38	450	19790101	20171231	7.8 [A]	12.7 [A]	n.n.	n.n.	14.7 [A]	n.n.	n.n.	n.n.
L06-1	con1	3231	Meiningen	50.56	10.38	450	19790101	20171231	7.8 [A]	12.7 [A]	n.n.	n.n.	14.7 [A]	n.n.	n.n.	n.n.
L06-2	con2	3231	Meiningen	50.56	10.38	450	19790101	20171231	7.8 [A]	12.7 [A]	n.n.	n.n.	14.7 [A]	n.n.	n.n.	n.n.
L07	dec	2667	Köln-Bonn	50.86	7.16	92	19600101	20171231	10.1 [A]	14.4 [A]	n.n.	n.n.	16.7 [A]	n.n.	n.n.	n.n.
L07	grass	2667	Köln-Bonn	50.86	7.16	92	19600101	20171231	10.1 [A]	14.4 [A]	n.n.	n.n.	16.7 [A]	n.n.	n.n.	n.n.
L08	con	2483	Kahler Asten	51.18	8.49	839	19510101	20171231	5.3 [A]	9.6 [A]	n.n.	n.n.	10.9 [A]	n.n.	n.n.	n.n.
L08	dec	2483	Kahler Asten	51.18	8.49	839	19510101	20171231	5.3 [A]	9.6 [A]	n.n.	n.n.	10.9 [A]	n.n.	n.n.	n.n.
L08	grass	2483	Kahler Asten	51.18	8.49	839	19510101	20171231	5.3 [A]	9.6 [A]	n.n.	n.n.	10.9 [A]	n.n.	n.n.	n.n.
L09	dec	2014	Hannover	52.46	9.68	55	19490101	20171231	9.2 [A]	13.7 [A]	n.n.	n.n.	15.9 [A]	n.n.	n.n.	n.n.
L09	grass	2014	Hannover	52.46	9.68	55	19490101	20171231	9.2 [A]	13.7 [A]	n.n.	n.n.	15.9 [A]	n.n.	n.n.	n.n.
L10	dec	691	Bremen	53.05	8.80	4	19490101	20171231	9.2 [A]	13.6 [A]	n.n.	n.n.	15.7 [A]	n.n.	n.n.	n.n.
L11	con	4466	Schleswig	54.53	9.55	43	19510101	20171231	8.4 [A]	12.6 [A]	n.n.	n.n.	14.4 [A]	n.n.	n.n.	n.n.
L11	grass	4466	Schleswig	54.53	9.55	43	19510101	20171231	8.4 [A]	12.6 [A]	n.n.	n.n.	14.4 [A]	n.n.	n.n.	n.n.
L12	dec	06120	Odense Lufthavn	55.48	10.33	15	19610101	20001231	8.3 [C,D]	12.5 [C,D]	n.n.	n.n.	n.a.	n.n.	n.n.	n.n.
L13	con	30110	Spodsbjerg	55.98	11.85	34	19610101	19901231	8.0 [C]	12.5 [C]	n.n.	n.n.	n.a.	n.n.	n.n.	n.n.
L13	dec	30110	Spodsbjerg	55.98	11.85	34	19610101	19901231	8.0 [C]	12.5 [C]	n.n.	n.n.	n.a.	n.n.	n.n.	n.n.
L14	con	74180	Hagshult Mo	57.29	14.13	169	19430101	20180601	5.8 [F]	10.8 [F]	19490101	20180601	14.5 [F]	n.n.	n.n.	n.n.
L15	con	84580	Snavlunda	58.97	14.90	144/140	19440101	19830901	5.4 [F]	10.8 [F]	19941014	19830831	13.9 [F]	85460	Kettstaka A	58.72
L15-1	dec1	84580	Snavlunda	58.97	14.90	144/140	19440101	19830901	5.4 [F]	10.8 [F]	19941014	19830831	13.9 [F]	85460	Kettstaka A	58.72
L15-2	dec2	84580	Snavlunda	58.97	14.90	144/140	19440101	19830901	5.4 [F]	10.8 [F]	19941014	19830831	13.9 [F]	85460	Kettstaka A	58.72
L16	dec	85330	Motala Kraftverk	58.55	15.08	94	19340101	19901228	6.4 [F]	11.6 [F]	19610101	19851024	14.9 [F]	84310	Karlsborg Mo	58.51

n.n. = not needed/see information further left

n.a. = not available

[A] DWD Climate Data Center, 2018a. Historical hourly station observations of 2m air temperature and humidity for Germany, version v006.

[B] DWD Climate Data Center, 2018b. Historical annual precipitation observations for Germany, version v007.

[C] Laursen, E.V., Thomsen, R.S., Cappelen, J., 1999. Observed Air Temperature, Humidity, Pressure, Cloud Cover and Weather in Denmark - with Climatological Standard Normals, 1961-90.

[D] Cappelen, J., 2002. Danish Climatological Normals 1971-2000 - for selected stations.

[E] Frich, P., Rosenørn, S., Madsen, H., Jensen, J.J., 1997. Observed Precipitation in Denmark, 1961-90.

[F] Swedish Meteorological and Hydrological Institute, 2018. SMHI Open Data Meteorological Observations, https://opendata-download-metobs.smhi.se/explore/.

Tab. S2. continuation…

Longitude (decimal °)	Altitude (m)	Oberservation begin (YYYYMMDD)	Oberservation end (YYYYMMDD)	RH_{MA} (%)	RH_{MV} (%)	RH_{MDV} (%)	Name	Latitude (decimal °)	Longitude (decimal °)	Altitude (m)	Oberservation begin (YYYYMMDD)	Oberservation end (YYYYMMDD)	P_{MA} (mm)	Source
n.n.	n.n.	n.n.	n.n.	82 [A]	80 [A]	70 [A]	n.n.	n.n.	n.n.	n.n.	n.n.	n.n.	1769 [B]	DWD
n.n.	n.n.	n.n.	n.n.	82 [A]	80 [A]	70 [A]	n.n.	n.n.	n.n.	n.n.	n.n.	n.n.	1769 [B]	DWD
n.n.	n.n.	n.n.	n.n.	78 [A]	77 [A]	73 [A]	n.n.	n.n.	n.n.	n.n.	n.n.	n.n.	1173 [B]	DWD
n.n.	n.n.	n.n.	n.n.	77 [A]	73 [A]	63 [A]	n.n.	n.n.	n.n.	n.n.	n.n.	n.n.	758 [B]	DWD
n.n.	n.n.	n.n.	n.n.	77 [A]	73 [A]	63 [A]	n.n.	n.n.	n.n.	n.n.	n.n.	n.n.	758 [B]	DWD
n.n.	n.n.	n.n.	n.n.	77 [A]	74 [A]	65 [A]	n.n.	n.n.	n.n.	n.n.	n.n.	n.n.	816 [B]	DWD
n.n.	n.n.	n.n.	n.n.	77 [A]	74 [A]	65 [A]	n.n.	n.n.	n.n.	n.n.	n.n.	n.n.	816 [B]	DWD
n.n.	n.n.	n.n.	n.n.	75 [A]	71 [A]	61 [A]	n.n.	n.n.	n.n.	n.n.	n.n.	n.n.	658 [B]	DWD
n.n.	n.n.	n.n.	n.n.	79 [A]	75 [A]	67 [A]	n.n.	n.n.	n.n.	n.n.	n.n.	n.n.	660 [B]	DWD
n.n.	n.n.	n.n.	n.n.	79 [A]	75 [A]	67 [A]	n.n.	n.n.	n.n.	n.n.	n.n.	n.n.	660 [B]	DWD
n.n.	n.n.	n.n.	n.n.	79 [A]	75 [A]	67 [A]	n.n.	n.n.	n.n.	n.n.	n.n.	n.n.	660 [B]	DWD
n.n.	n.n.	n.n.	n.n.	77 [A]	74 [A]	65 [A]	n.n.	n.n.	n.n.	n.n.	n.n.	n.n.	809 [B]	DWD
n.n.	n.n.	n.n.	n.n.	77 [A]	74 [A]	65 [A]	n.n.	n.n.	n.n.	n.n.	n.n.	n.n.	809 [B]	DWD
n.n.	n.n.	n.n.	n.n.	87 [A]	84 [A]	78 [A]	n.n.	n.n.	n.n.	n.n.	n.n.	n.n.	1417 [B]	DWD
n.n.	n.n.	n.n.	n.n.	87 [A]	84 [A]	78 [A]	n.n.	n.n.	n.n.	n.n.	n.n.	n.n.	1417 [B]	DWD
n.n.	n.n.	n.n.	n.n.	87 [A]	84 [A]	78 [A]	n.n.	n.n.	n.n.	n.n.	n.n.	n.n.	1417 [B]	DWD
n.n.	n.n.	n.n.	n.n.	80 [A]	76 [A]	68 [A]	n.n.	n.n.	n.n.	n.n.	n.n.	n.n.	650 [B]	DWD
n.n.	n.n.	n.n.	n.n.	80 [A]	76 [A]	68 [A]	n.n.	n.n.	n.n.	n.n.	n.n.	n.n.	650 [B]	DWD
n.n.	n.n.	n.n.	n.n.	80 [A]	77 [A]	69 [A]	n.n.	n.n.	n.n.	n.n.	n.n.	n.n.	699 [B]	DWD
n.n.	n.n.	n.n.	n.n.	83 [A]	80 [A]	72 [A]	n.n.	n.n.	n.n.	n.n.	n.n.	n.n.	900 [B]	DWD
n.n.	n.n.	n.n.	n.n.	83 [A]	80 [A]	72 [A]	n.n.	n.n.	n.n.	n.n.	n.n.	n.n.	900 [B]	DWD
n.n.	n.n.	19800101	19971231	81 [C]	76 [C]	63 [C]	n.n.	n.n.	n.n.	n.n.	n.n.	n.n.	572 [E]	DMI
n.n.	n.n.	19690101	19921231	84 [C]	80 [C]	74 [C]	n.n.	n.n.	n.n.	n.n.	n.n.	n.n.	554 [E]	DMI
n.n.	n.n.	19690101	19921231	84 [C]	80 [C]	74 [C]	n.n.	n.n.	n.n.	n.n.	n.n.	n.n.	554 [E]	DMI
n.n.	n.n.	20130101	20180601	86 [F]	79 [F]	68 [F]	n.n.	n.n.	n.n.	n.n.	19430101	20180601	717 [F]	SMHI
15.03	225	19950801	20180601	82 [F]	75 [F]	68 [F]	Snavlunda D	58.95/58.97/58.97	14.91/14.90/14.90	135/144/140	19440101	20150101	693 [F]	SMHI
15.03	225	19950801	20180601	82 [F]	75 [F]	68 [F]	Snavlunda D	58.95/58.97/58.97	14.91/14.90/14.90	135/144/140	19440101	20150101	693 [F]	SMHI
15.03	225	19950801	20180601	82 [F]	75 [F]	68 [F]	Snavlunda D	58.95/58.97/58.97	14.91/14.90/14.90	135/144/140	19440101	20150101	693 [F]	SMHI
14.51	95	20130101	20180601	83 [F]	78 [F]	71 [F]	Motala	58.56/58.55/58.55	15.02/15.01/15.08	95/95/94	19310101	20180501	557 [F]	SMHI

Tab. S3. GDGT data. Crenarcheol and brGDGTs in µg/g dry weight.

Location	Vegetation	pH (H_2O)	Crenarcheol [A]	IIIa [A]	IIIb [A]	IIIc [A]	IIa [A]	IIb [A]	IIc [A]	Ia [A]	Ib [A]	Ic [A]
			(ng/g dry weight)	(ng/g dry weight)	(ng/g dry weight)	(ng/g dry weight)	(ng/g dry weight)	(ng/g dry weight)	(ng/g dry weight)	(ng/g dry weight)	(ng/g dry weight)	(ng/g dry weight)
L01	con	4.5	2	194	3	0	845	34	1	531	38	7
L01	dec	4.0	1	109	1	0	536	7	3	687	37	10
L02	con	6.5	38	128	9	1	329	81	4	160	86	79
L03	dec	4.3	16	55	0	0	617	17	5	1289	30	9
L03	grass	5.2	12	28	0	0	142	8	1	124	12	2
L04	dec	5.9	13	60	4	1	185	37	3	137	33	6
L04	grass	6.0	208	54	7	3	131	105	8	79	92	27
L05	dec	4.1	15	25	0	0	204	2	1	380	5	1
L06	dec	7.3	16	226	26	1	304	184	6	78	66	5
L06-1	con1	4.5	2	116	0	0	585	18	2	549	21	1
L06-2	con2	6.0	19	332	24	2	695	197	7	295	97	12
L07	dec	3.6	149	67	1	1	506	10	4	677	16	5
L07	grass	4.2	18	19	0	0	141	1	1	183	2	1
L08	con	3.3	29	213	0	0	2265	26	19	3287	32	13
L08	dec	3.6	11	84	0	0	821	12	5	1450	21	8
L08	grass	4.3	0	232	0	0	996	11	2	884	21	6
L09	dec	3.6	64	101	1	0	943	13	5	1513	19	8
L09	grass	4.3	16	26	1	0	169	1	1	275	5	1
L10	dec	3.0	1084	157	33	4	463	68	17	816	23	8
L11	con	3.5	512	76	0	1	353	6	0	406	8	2
L11	grass	5.9	19	89	0	0	579	26	2	714	44	5
L12	dec	4.9	735	450	16	2	2219	418	36	1642	476	142
L13	con	3.2	0	56	0	3	619	0	6	993	13	20
L13	dec	3.7	0	150	0	0	1422	28	16	3165	46	19
L14	con	3.6	0	103	2	0	1180	5	9	2077	17	4
L15	con	3.6	0	207	3	1	2866	48	26	5695	98	35
L15-1	dec1	5.0	7	192	2	0	933	41	4	658	58	22
L15-2	dec2	4.1	5	210	1	0	1896	24	14	2541	41	13
L16	dec	4.3	0	54	0	0	349	5	1	424	9	2

[A] structures can be found in Fig. S5

[B] BIT index was calculated according to Hopmans, E.C., Weijers, J.W.H., Schefuß, E., Herfort, L., Sinninghe Damsté, J.S., Schouten, S., 2004. A novel proxy for terrestrial organic matter in sediments based on branched and isoprenoid tetraether lipids. Earth and Planetary Science Letters 224, 107–116.

[C] MBT', CBT, reconstructed T_{MA} and pHCBT according to Peterse, F., van der Meer, J., Schouten, S., Weijers, J.W.H., Fierer, N., Jackson, R.B., Kim, J.H., Sinninghe Damsté, J.S., 2012. Revised calibration of the MBT-CBT paleotemperature proxy based on branched tetraether membrane lipids in surface soils. Geochimica et Cosmochimica Acta 96, 215–229.

Tab. S3. continuation…

brGDGT concentration (µg/g dry weight)	BIT	MBT'	CBT	reconstructed T_{MA} (°C)	pH_{CBT}
1.65	1.00	0.35	1.3	4.3	5.37
1.39	1.00	0.53	1.4	9.0	5.05
0.88	0.94	0.37	0.5	9.8	6.98
2.02	0.99	0.66	1.6	12.1	4.74
0.32	0.96	0.43	1.1	7.9	5.69
0.47	0.97	0.38	0.7	8.9	6.59
0.51	0.56	0.40	0.0	13.0	7.84
0.62	0.98	0.63	2.0	9.0	4.01
0.90	0.97	0.17	0.2	5.1	7.54
1.29	1.00	0.44	1.5	6.3	5.04
1.66	0.99	0.25	0.5	5.5	6.86
1.29	0.89	0.54	1.7	8.2	4.63
0.35	0.95	0.53	2.0	5.9	3.90
5.86	1.00	0.57	2.0	7.2	4.00
2.40	1.00	0.62	1.8	9.4	4.26
2.15	1.00	0.42	1.8	3.8	4.39
2.60	0.98	0.59	1.9	8.5	4.19
0.48	0.97	0.59	1.9	8.5	4.23
1.59	0.57	0.55	1.2	11.2	5.63
0.85	0.62	0.49	1.7	6.2	4.50
1.46	0.99	0.52	1.3	9.8	5.40
5.40	0.85	0.42	0.6	10.2	6.65
1.71	1.00	0.60	2.1	7.6	3.78
4.85	1.00	0.67	1.8	11.3	4.37
3.40	1.00	0.62	2.2	7.7	3.64
8.98	1.00	0.65	1.8	10.9	4.42
1.91	1.00	0.39	1.2	6.0	5.52
4.74	1.00	0.55	1.8	7.4	4.29
0.84	1.00	0.52	1.7	6.9	4.46

Tab. S4. Measured *n*-alkane δ^2H and sugar $\delta^{18}O$ data along with calculations and reconstruction results.

Location	Vegetation	*n*-alkane δ^2H (‰)	sugar $\delta^{18}O$ (‰)	$\varepsilon_{n\text{-alkane/precipitation}}$ (‰)	$\varepsilon_{sugar/precipitation}$ (‰)	reconstructed $\delta^2H_{source\text{-}water}$ (‰)	reconstructed $\delta^{18}O_{source\text{-}water}$ (‰)	reconstructed RH_{MDV} (‰)
L01	con	-216.2	34.17	-149	45.5	-139	-18.7	34
L01	dec	-190.6	35.95	-121	47.3	-100	-13.8	42
L02	con	-169.4	32.95	-103	43.7	-49	-7.3	66
L03	dec	-176.8	34.54	-127	42.8	-67	-9.6	56
L03	grass	n.a.	29.96	n.a.	38.1	n.a.	n.a.	n.a.
L04	dec	n.a.	35.30	n.a.	43.7	n.a.	n.a.	n.a.
L04	grass	-208.6	30.80	-160	39.2	-110	-14.9	52
L05	dec	-169.6	32.95	-121	41.1	-47	-7.1	66
L06	dec	n.a.	34.30	n.a.	43.9	n.a.	n.a.	n.a.
L06-1	con1	-201.5	34.27	-146	43.9	-113	-15.3	42
L06-2	con2	-191.0	34.39	-135	44.0	-94	-13.0	48
L07	dec	-170.4	36.07	-124	43.8	-62	-9.0	54
L07	grass	n.a.	31.28	n.a.	39.2	n.a.	n.a.	n.a.
L08	con	-168.3	38.42	-113	48.1	-72	-10.2	45
L08	dec	-156.3	36.19	-101	45.8	-40	-6.2	61
L08	grass	-184.2	31.51	-130	41.1	-71	-10.1	63
L09	dec	-177.8	31.66	-129	39.8	-57	-8.4	66
L09	grass	-191.6	28.30	-144	36.4	-69	-9.8	71
L10	dec	-171.6	39.45	-126	47.3	-79	-11.1	40
L11	con	-183.6	33.56	-135	41.8	-77	-10.8	55
L11	grass	-194.1	27.67	-146	35.8	-71	-10.1	72
L12	dec	-177.4	37.30	-124	46.4	-83	-11.6	44
L13	con	-182.9	36.62	-124	46.6	-90	-12.5	44
L13	dec	-183.8	28.79	-125	38.7	-57	-8.4	74
L14	con	-190.3	36.85	-128	47.4	-103	-14.1	39
L15	con	-201.1	32.13	-135	43.3	-103	-14.1	51
L15-1	dec1	-201.6	33.41	-136	44.6	-110	-15.0	45
L15-2	dec2	-209.7	33.05	-145	44.2	-123	-16.6	42
L16	dec	-191.6	28.41	-128	39.2	-69	-9.9	71

n.a. = not available